Equilibrium Beach Profiles: Characteristics and Applications

Robert G. Dean

Coastal and Oceanographic Engineering Department
University of Florida
336 Weil Hall
Gainesville, FL 32611, USA

ABSTRACT ■

DEAN, R.G., 1990. Equilibrium beach profiles: characteristics and applications. *Journal of Coastal Research*, 7(1), 53–84. Fort Lauderdale (Florida), ISSN 0749-0208.

An understanding of equilibrium beach profiles can be useful in a number of types of coastal engineering projects. Empirical correlations between a scale parameter and the sediment size or fall velocity allow computation of equilibrium beach profiles. The most often used form is $h(y) = Ay^{2/3}$ in which h is the water depth at a distance y from the shoreline and A is the sediment-dependent scale parameter. Expressions for shoreline position change are presented for arbitrary water levels and wave heights. Application of equilibrium beach profile concepts to profile changes seaward of a seawall include effects of sea level change and arbitrary wave heights. For fixed wave heights and increasing water level, the additional depth adjacent to the seawall first increases, then decreases to zero for a wave height just breaking at the seawall. Shoreline recession and implications due to increased sea level and wave heights are examined. It is shown, for the equilibrium profile form examined, that the effect of wave set-up on recession is small compared to expected storm tides during storms. Profile evolution from a uniform slope is shown to result in five different profile types, depending on initial slope, sediment characteristics, berm height and depth of active sediment redistribution. The reduction in required sand volumes through perching of a nourished beach by an offshore sill is examined for arbitrary sediment and sill combinations. When beaches are nourished with a sediment of arbitrary but uniform size, it is found that three types of profiles can result: (1) submerged profiles in which the placed sediment is of smaller diameter than the native and all of the sediment equilibrates underwater with no widening of the dry beach, (2) non-intersecting profiles in which the seaward portion of the placed material lies above the original profile at that location, and (3) intersecting profiles with the placed sand coarser than the native and resulting in the placed profile intersecting with the original profile. Equations and graphs are presented portraying the additional dry beach width for differing volumes of sand of varying sizes relative to the native. The offshore volumetric redistribution of material due to sea level rise as a function of water depth is of interest in interpreting the cause of shoreline recession. If only offshore transport occurs and the surveys extend over the active profile, the net volumetric change is zero. It is shown that the maximum volume change due to cross-shore sediment redistribution is only a fraction of the product of the active vertical profile dimension and shoreline recession. The paper presents several other applications of equilibrium beach profiles to problems of coastal engineering interest.

ADDITIONAL INDEX WORDS: *Beach erosion, nourishment, sea level rise, seawalls.*

INTRODUCTION

A quantitative understanding of the characteristics of equilibrium beach profiles is central to rational design of many coastal engineering projects and to the interpretation of nearshore processes. Several features of equilibrium beach profiles are well-known: (1) they tend to be concave upwards, (2) smaller and larger sand diameters are associated with milder and steeper slopes, respectively, (3) the beach face is approximately planar, and (4) steep waves result in milder slopes and a tendency for bar formation.

In a broad sense, it is obvious that sand particles are acted upon by a complex system of constructive and destructive generic "forces" with the constructive forces acting to displace the sediment particle landward and vice versa. Constructive forces include landward directed bottom shear stresses due to the nonlinear character of shallow water waves, landward directed "streaming" velocities in the bottom boundary layer (BAGNOLD, 1946; PHILLIPS, 1966), the phasing associated with intermittent suspended sediment motion, *etc.* The most obvious destructive force is that of gravity coupled with the destabilizing effects of turbulence induced by wave-breaking; others include the

effect of seaward directed bottom undertow currents and forces due to wave set-up within the surf zone (*e.g.* SVENDSEN, 1984; STIVE and WIND, 1986). Indeed, the above represents only a partial listing of the complex force system acting on sediment particles and serves to illustrate the difficulty of a rational physics-based prediction of equilibrium beach profiles.

Several approaches have been pursued in an attempt to characterize equilibrium beach profiles. KEULEGAN and KRUMBEIN (1949) investigated the characteristics of a mild bottom slope such that the waves never break but rather are continually dissipated by energy losses due to bottom friction. BRUUN (1954) analyzed beach profiles from the Danish North Sea coast and Mission Bay, California, and found that they followed the simple relationship

$$h(y) = Ay^{2/3} \qquad (1)$$

in which h is the water depth at a seaward distance, y, and A is a scale parameter which depends primarily on sediment characteristics. EAGLESON, GLENNE and DRACUP (1963) developed a complex characterization of the wave and gravity forces acting on a particle located outside the zone of "appreciable breaker influence" and developed expressions for the seaward limit of motion and for the beach slope for which a sand particle would be in equilibrium.

SWART (1974) carried out a series of wave tank tests and developed empirical expressions relating profile geometry and transport characteristics to the wave and sediment conditions. The active beach profile was divided into four zones and empirical expressions were developed for each zone. VELLINGA (1983) investigated dune erosion using wave tank tests and developed the following "erosion profile" which included the effect of deep water significant wave height, H_{os}, and sediment fall velocity, w,

$$\left(\frac{7.6}{H_{OS}}\right)h = 0.47\left[\left(\frac{7.6}{H_{OS}}\right)^{1.28}\left(\frac{w}{.0268}\right)^{0.56}y+18\right] - 2.0 \qquad (2)$$

in which the values of all variables are in the metric system. It can be shown that Eq. (2) is in reasonably good agreement with Eq. (1). SUNAMURA and HORIKAWA (1974) examined and characterized beach profiles for two sizes of sed-

iments, and ranges of wave heights and periods and initial slopes of planar beaches. Three beach profile types were established in laboratory experiments including one erosional and two accretional types. SUH and DALRYMPLE (1988) applied concepts of equilibrium beach profiles to address the same problem as Sunamura and Horikawa and identified one erosional profile type and one accretional type. Comparison of laboratory data demonstrated good agreement with their criteria and predictions of profile changes.

Numerous investigations have been carried out to develop appropriate scale modeling criteria including DALRYMPLE and THOMPSON (1976), NODA (1972), HUGHES (1983) and VAN HIJUM (1975). HAYDEN *et al.* (1975) apparently were the first to apply the concept of empirical orthogonal functions (EOF) to extract the principal modes of change from a set of beach profile data. Numerous later studies have used this approach to investigate the character of the dominant modes of profile change, *e.g.* WINANT *et al.* (1975), WEISHAR and WOOD (1983), AUBREY *et al.* (1977), and AUBREY (1979). The EOF is a purely descriptive method and does not address the causes or processes of profile change.

HAYDEN *et al.* (1975) assembled a data set comprising 504 beach profiles along the Atlantic and Gulf coasts of the United States. DEAN (1977) analyzed these profiles and used a least squares procedure to fit an equation of the form

$$h = Ay^n \qquad (3)$$

to the data and found a central value of $n = \frac{2}{3}$ as BRUUN had earlier. It was shown that Eq. (3) with $n = \frac{2}{3}$ is consistent with uniform wave energy dissipation per unit volume, $\mathscr{D}_*$, within the breaking zone, i.e.,

$$\mathscr{D}_* = \frac{1}{h}\frac{\partial}{\partial y}(EC_G) \qquad (4)$$

where E and C_G are the wave energy density and group velocity, respectively. It can be shown from linear shallow water wave theory that $\mathcal{D}_*$ and A are related by

$$A = \left[\frac{24\mathscr{D}_*(D)}{5\rho g^{3/2}\kappa^2}\right]^{2/3} \qquad (5)$$

in which E is the wave energy density, C_G is the group velocity, ρ is the water mass density, g is

gravity, D is sediment particle diameter and κ is a constant relating wave height to water depth within the surf zone. The interpretation of Eq. (3) is that a particle of given size is characterized by an associated stability and that the wave breaking process results in the transformation of organized wave motion into chaotic turbulence fluctuations; these fluctuations are destructive forces and, if too great, cause mobilization of the sediment particle with resulting offshore displacement and a milder beach slope, which reduces the wave energy dissipation per unit volume eventually resulting in an equilibrium profile. Later MOORE (1982) collected and analyzed a number of published beach profiles and developed the relationship between A and D as shown by the solid line in Figure 1. As expected, the larger the sediment size, the greater the A parameter and the steeper the beach slope. Figures 2, 3 and 4 present several profiles employed by Moore in establishing the relationship presented in Figure 1. The profile in Figure 2 is of particular interest as the sediment particle size ranges from 15 cm to 30 cm, approximately the size of bowling balls! DEAN (1987a) has shown that when the relationship presented in Figure 1 is transformed to $A(w)$ rather than $A(D)$, where w is the fall velocity, the relationship is surprisingly linear (on a log-

log plot) as presented by the dashed line in Figure 1.

KRIEBEL (1982), KRIEBEL and DEAN (1984, 1985) and KRIEBEL (1986) have considered profiles out of equilibrium by hypothesizing that the offshore transport is proportional to the difference between the actual and equilibrium wave energy dissipation per unit volume, i.e.

$$Q = K(\mathscr{D} - \mathscr{D}_*) \qquad (6)$$

Eq. (6) and a sand conservation relationship have been incorporated into a numerical model of sediment transport with generally good confirmation between laboratory profiles (Figure 5) and field results (Figure 6). LARSON (1988) and LARSON and KRAUS (1989) have considered the active region of sediment transport in four zones and have developed empirical counterparts to Eq. (6) for each zone, thus allowing solution of the transient beach profile problem including a capability for generating longshore bars.

MODIFIED EQUILIBRIUM BEACH PROFILE

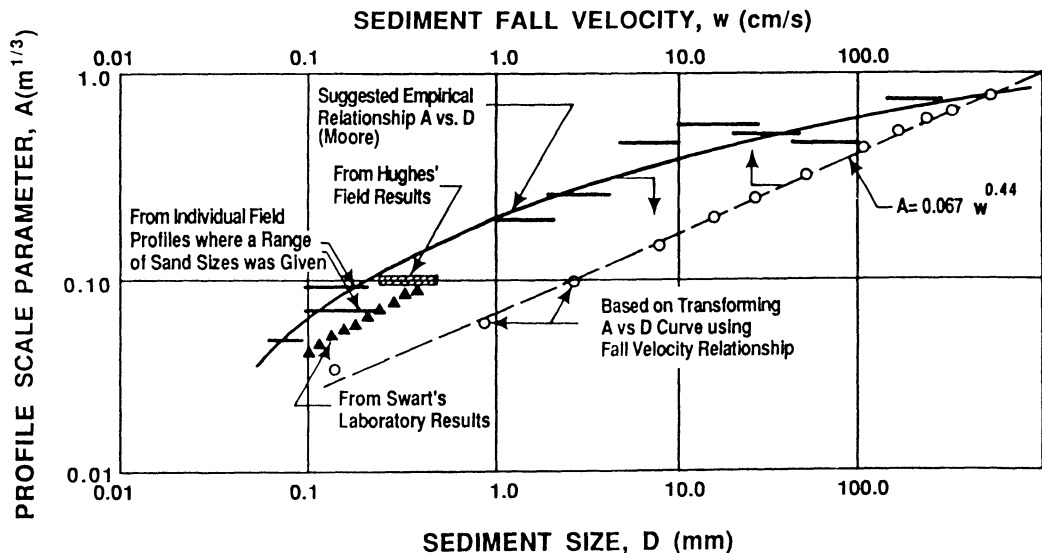An unrealistic property of the form of the equilibrium beach profile represented by Eq. (1)

Figure 1. Beach profile factor, A, vs sediment diameter, D, and Fall velocity, w, in relationship $h = Ax^{2/3}$ (Dean, 1987a; modified from Moore, 1982).
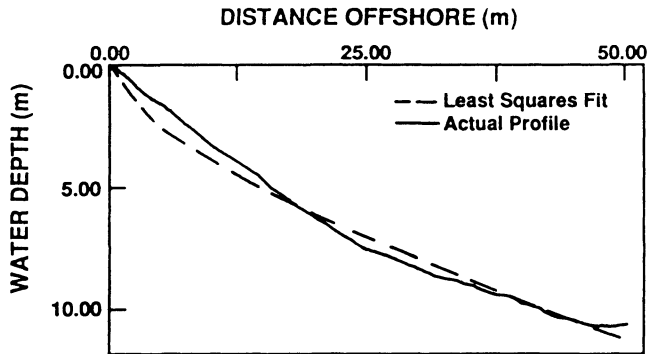
DISTANCE OFFSHORE (m)

Figure 2.   Profile P4 from Zenkovich (1967). A boulder coast in Eastern Kamchatka. Sand diameter: 150mm–300 mm. Least squares value of $A = 0.82$ m$^{1/3}$ (from Moore, 1982).
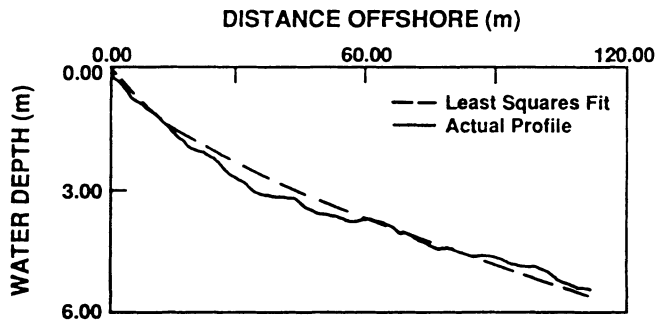
DISTANCE OFFSHORE (m)

Figure 3.   Profile P10 from Zenkovich (1967). Near the end of a spit in western Black Sea. Whole and broken shells. $A = 0.25$ m$^{1/3}$ (from Moore, 1982).

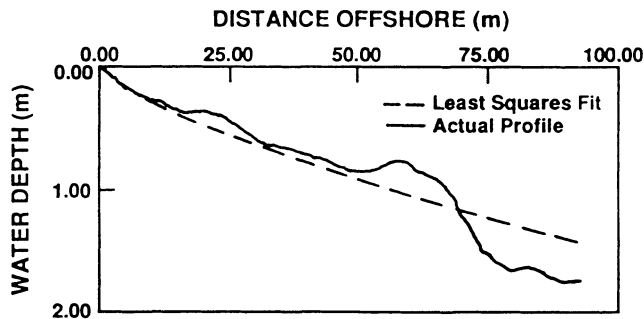DISTANCE OFFSHORE (m)

Figure 4.   Profile from Zenkovich (1967). Eastern Kamchatka. Mean sand diameter: 0.25 mm. Least squares value of $A = 0.07$ m$^{1/3}$ (from Moore, 1982).
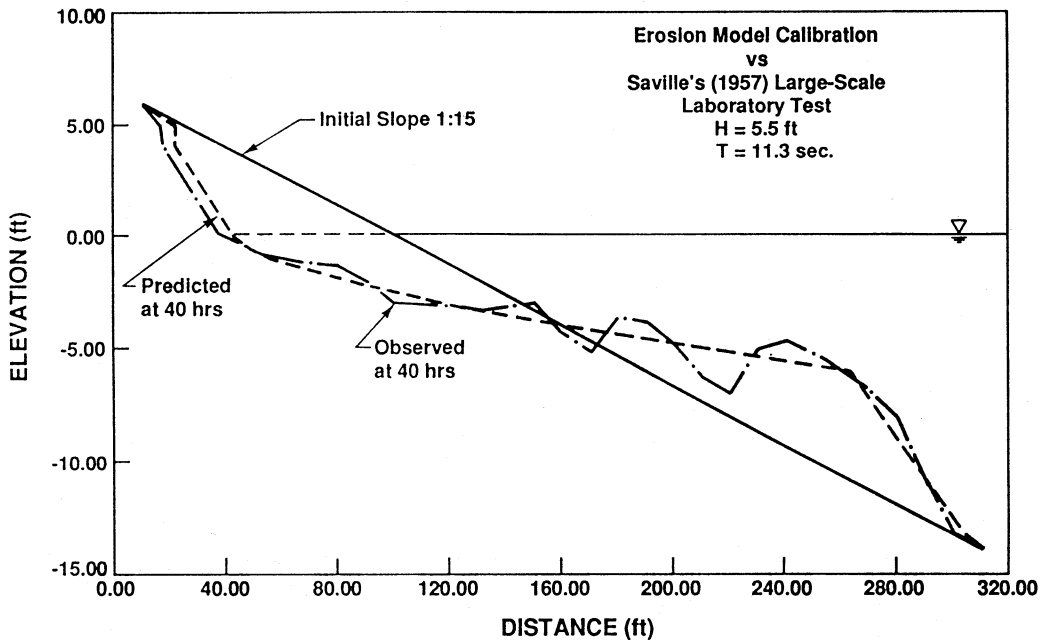
Figure 5. Comparison of calibrated profile response model with large wave tank data by Saville (1957) (from Kriebel, 1986).
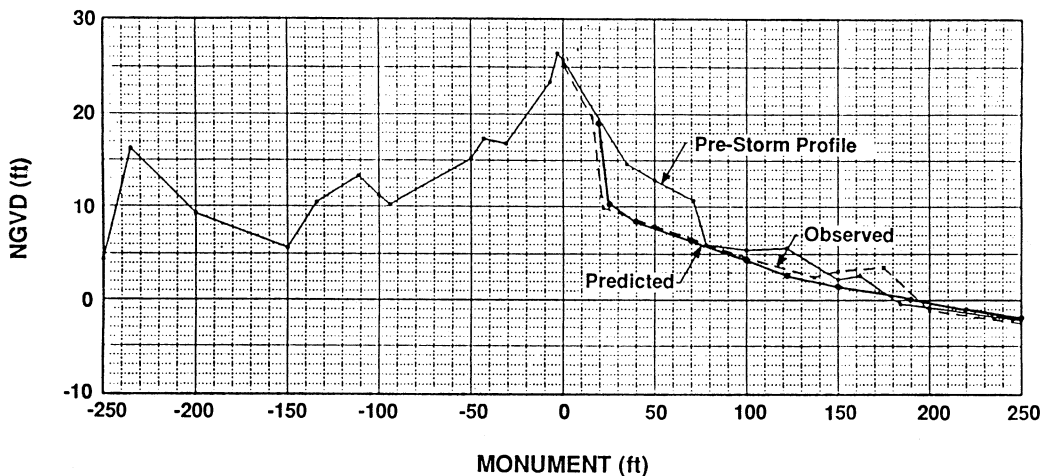

Figure 6. Comparison of calibrated profile response model with field profile affected by Hurricane Eloise as reported by Chiu (1977) (from Kriebel, 1986).

is the predicted infinite slope at the shoreline. Large slopes induce correspondingly large gravity forces which are not represented in Eq.

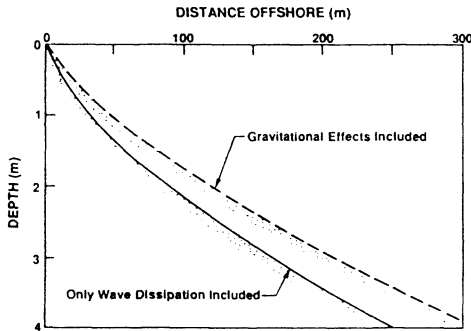(1). A slight modification to include gravitational effects is

Figure 7. Comparison of equilibrium beach profile with and without gravitational effects included. $A = 0.1$ m$^{1/3}$ corresponding to a sand size of 0.2 mm.

Figure 8. Definition sketch for profile response due to sea level rise.

$$\frac{\mathcal{D}_*}{m}\frac{\partial h}{\partial y} + \frac{1}{h}\frac{\partial}{\partial y}(EC_G) = \mathcal{D}_* \qquad (7)$$

Gravity Effect   Turbulence Effect

in which the two terms on the left hand size represent destabilizing forces due to gravity and turbulent fluctuations due to wave energy dissipation, m is the beach face slope, and as before $\mathcal{D}_*$ represents the stability characteristics of the sediment particle but now the interpretation of $\mathcal{D}_*$ is broadened beyond equilibrium energy dissipation per unit volume to include gravity as an additional destabilizing force. Eq. (7) can be integrated to:

$$y = \frac{h}{m} + \frac{1}{A^{3/2}}h^{3/2} \qquad (8)$$

where, as before, A is related to $\mathcal{D}_*$ by Eq. (5). In shallow water, the first term in Eq. (8) dominates, simplifying to

$$h = my \qquad (9)$$

i.e. the beach face is of uniform slope, m, consistent with measurements in nature. In deeper water, the second term in Eq. (8) dominates with the following simplification

$$h = Ay^{2/3} \qquad (10)$$

as presented earlier.

Figure 7 presents a comparison of Eq. (8), which includes the planar portion near the water line and Eq. (1) which has an infinite slope at the water line. A form similar to Eq. (8) was adopted by LARSON (1988) and LARSON and KRAUS (1989).
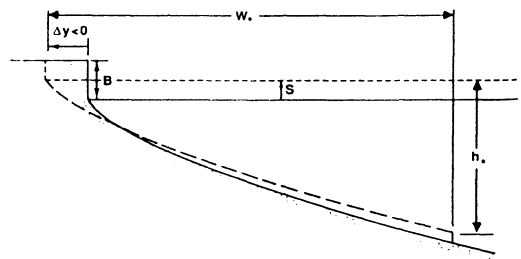
APPLICATIONS OF EQUILIBRIUM BEACH PROFILES OF THE FORM: $h = Ay^{2/3}$

The utility of Eq. (1) will be illustrated by several examples. A definition sketch of the system of interest is presented as Figure 8. In results presented here, it will be assumed that within the surf zone the wave height is proportional to the local water depth with the proportionality factor, κ, i.e. $H = \kappa h (\kappa \approx 0.78)$. In particular, the breaking wave height, H_b, and breaking depth, h_*, are related by $H_b = \kappa h_*$.

Effect of Sediment Size on Beach Profile

Figure 9 presents two examples of the effect of sediment size on beach profile. The scale parameter A is determined for various sediment sizes from Figure 1 and the profiles computed from Eq. (1).

Beach Response to Altered Water Level and Waves

The effects of elevated and lowered water levels will be treated separately.

An elevated water level, S, with wave and sediment conditions such that the profile is reconfigured out to a depth, h_*, is assumed to result in equilibrium with the final state being the same profile form as before, but relative to the elevated water level. This situation could pertain to a storm tide of long duration or to sea level rise.

Referring to Figure 8, the sand volume eroded, V_E, is equal to the volume deposited, V_D
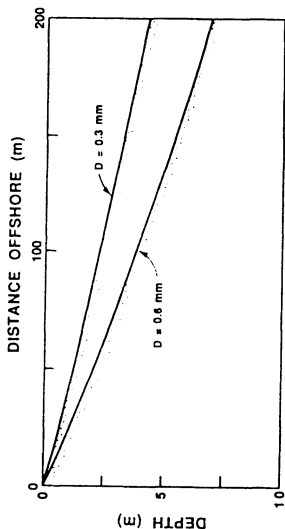
$$V_E = V_D \qquad (11)$$

Figure 9. Equilibrium beach profiles for sand sizes of 0.2 mm and 0.6 mm $A(D = 0.2 \text{ mm}) = 0.1 \text{ m}^{1/3}$, $A(D = 0.6 \text{ mm}) = 0.20$ $\text{m}^{1/3}$.

When Eqs. (1) and (11) are combined the following implicit equation for the shoreline change, Δy, is obtained

$$\Delta y + \frac{3}{5}\frac{h_*W_*}{B}\left(1 + \frac{\Delta y}{W_*}\right)^{5/3}$$
$$= \frac{3}{5}\frac{h_*W_*}{B} - \left(\frac{S}{B}W_*\right) \quad (12)$$

in which W_* is the seaward limit of the active profile $\left(W_* = \left(\frac{H_b}{\kappa A}\right)^{3/2}\right)$, B is the berm height and for this case of shoreline recession $\Delta y < 0$. Eq. (12) can be expressed in non-dimensional form as

$$\Delta y' - \frac{3}{5B'}[1 - (1+\Delta y')^{5/3}] + S' = 0 \quad (13)$$

in which the non-dimensional variables are

$$\Delta y' \equiv \frac{\Delta y}{W_*}$$
$$B' = \frac{B}{h_*} \quad (14)$$
$$S' = \frac{S}{B}$$

Eq. (13) is plotted in Figure 10. For small values of $\Delta y'$, Eq. (13) can be approximated by

$$\Delta y = -S\frac{W_*}{(h_*+B)} \quad (15)$$

first proposed by BRUUN (1962) and now referred to as the "Bruun Rule".

For the case of lowered water levels, there will be an excess of sand in the active system and a resulting advancement of the shoreline. The profile equilibration depth, h_*, will occur at a distance, W_2, from the original shoreline. This equilibrium depth is considered to extend as a horizontal terrace from the distance W_2 noted above to a landward location consistent with the equilibrium profile and the shoreline advance, Δy. For this case, shown in Figure 11, the non-dimensional shoreline advancement can be shown to be

$$\Delta y' = \frac{2}{5}\frac{(1 - S'B')^{5/2} - 1}{(B' - S'B' + 1)} \quad (16)$$

where it is emphasized that for this case, $S' < 0$. Additionally,

$$W'_2 = \frac{W_2}{W_*} = (1 - S'B')^{3/2} \quad (17)$$

and the landward location of the terrace, W_1, is

$$W'_1 = \frac{W_1}{W_*} = 1 + \Delta y' \quad (18)$$

The other non-dimensional parameters are as defined by Eqs. (14).

Equilibrium Profile and Recession Including the Effect of Wave Set-Up

The equilibrium beach profile, $h = Ay^{2/3}$, interpreted as resulting from uniform wave energy dissipation per unit water volume does not include the effect of wave set-up. As a precursor to developing recession predictions due to increased water levels and wave set-up, it is useful to first establish the equilibrium beach profile, including the effect of wave set-up, $\bar{\eta}$.

We start with the well-known solution for wave set-up across the surf zone (BOWEN et al., 1968)

$$\bar{\eta}(y) = \bar{\eta}_b + J[h_b - h(y)] \quad (19)$$

in which h_b is the breaking depth ($h_b = h_* - \bar{\eta}_b - S$), $\bar{\eta}_b$ is the set-up (actually negative) at breaking, and
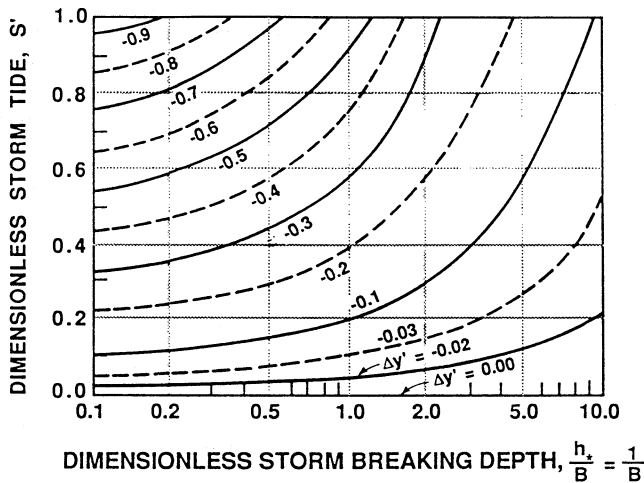
Figure 10. Isolines of dimensionless shoreline change, $\Delta y'$, vs dimensionless storm breaking depth, h'_*, and dimensionless storm tide, S'.
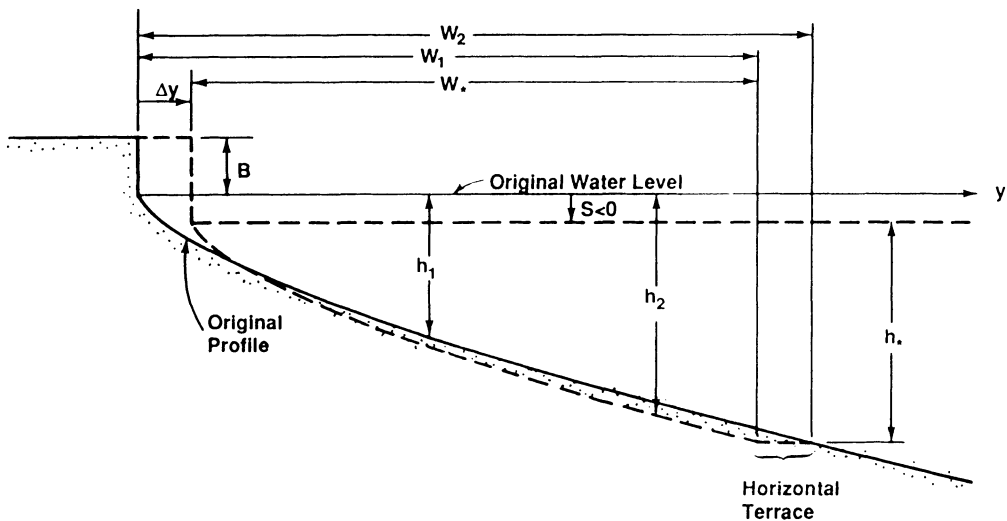

Figure 11. Profile geometry and notation for shoreline advancement due to lowering of water level.

$$J = \frac{3\kappa^2/8}{1+3\kappa^2/8} \qquad (20)$$

$$\overline{\eta}_b = -\frac{1}{8}\frac{kH_b^2}{\sinh 2kh_*} \qquad (21)$$

where k is the wave number. Since $\overline{\eta}$ is positive over most of the surf zone, it is reasonable that it contributes much like a tide in causing recession, especially for the larger breaking wave

heights. The equilibrium profile based on uniform wave energy dissipation per unit volume commences from

$$\left(\frac{1}{(h+S+\overline{\eta})}\right)\frac{\partial}{\partial y_l}(EC_G) = -\mathcal{D}_* \qquad (22)$$

in which y_l is directed landward, and as before E is the wave energy density, and C_G the group velocity. Assuming shallow water,

$$EC_G = \frac{\rho g}{8}\kappa^2(h+S+\overline{\eta})^2\sqrt{g(h+S+\overline{\eta})}$$

If the algebra is carried through, the not-too-surprising result is obtained

$$h+S+\overline{\eta} = Ay^{2/3} \qquad (23)$$

where the y-origin is now the location where $h+S+\overline{\eta} = 0$. Figure 12 presents a plot of the non-dimensional wave set-up and the associated equilibrium beach profile.

In the following development, the effects of a uniform storm tide, S, and the set-up which varies across the surf zone (Eq. (23)) will be considered as presented in Figure 13. Following procedures similar to those used for determining recession with a water level which is uniform across the surf zone, volumes are equated as

$$\int_{\Delta y}^{0} [B-S-\overline{\eta}(y)]dy + \int_{\Delta y}^{W_*+\Delta y} A(y-\Delta y)^{2/3}dy$$

$$= \int_{0}^{W_*+\Delta y} Ay^{2/3}dy + \int_{0}^{W_*+\Delta y} [S+\overline{\eta}(y)]dy \qquad (24)$$

which after considerable algebra yields

$$\Delta y' + \frac{3}{5B'}[1 + \Delta y']^{5/3}$$

$$= \frac{1}{B'}\frac{(3/5 - J)}{(1 - J)} - S' - \overline{\eta}'_b \qquad (25)$$

in which Eqs. (14) have been used for non-dimensionalization and $\eta'_b = \eta_b/B$.

The question of the relative roles of breaking waves and storm surges can be addressed by simplifying Eq. (25) for the case of relatively small non-dimensional beach recessions, $|\Delta y'| << 1$), which upon adoption of $\kappa = 0.78$ and expressing in dimensional form yields

$$\frac{\Delta y}{W_*} \approx -\frac{0.068\dfrac{H_b}{B} + \dfrac{S}{B}}{1 + 1.28\dfrac{H_b}{B}} \qquad (26)$$

It is necessary to exercise care in interpreting Eq. (26), as the surf zone width, W_* includes the effect of the breaking wave height,

$$W_* = \left(\frac{H_b}{\kappa A}\right)^{3/2} \qquad (27)$$

As shown by Eq. (26), the dimensionless beach change ($\Delta y/W_*$) is much more strongly related to storm surge than wave height with the storm surge being approximately 16 times as effective in causing the dimensionless beach recession. However, during storms the breaking wave height may be two to three times as great as the storm tide and the larger breaking waves may persist much longer than the peak storm tides. The reason that the storm tide plays a much greater role than that due to breaking wave set-up is evident from Figure 12 where it is seen that the wave set-up (actually the set-down)
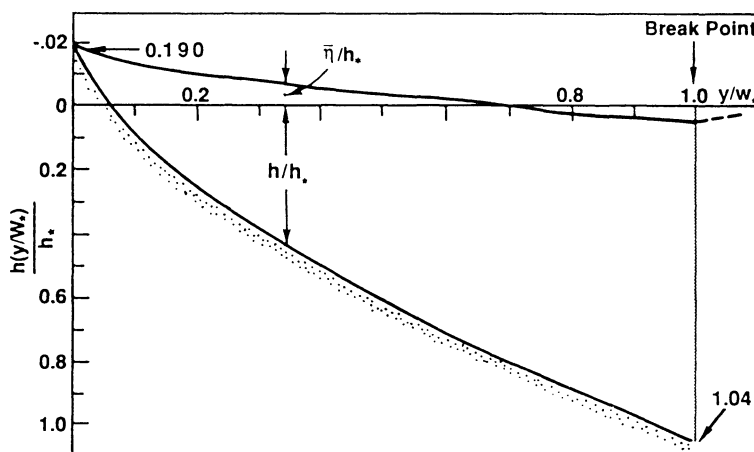

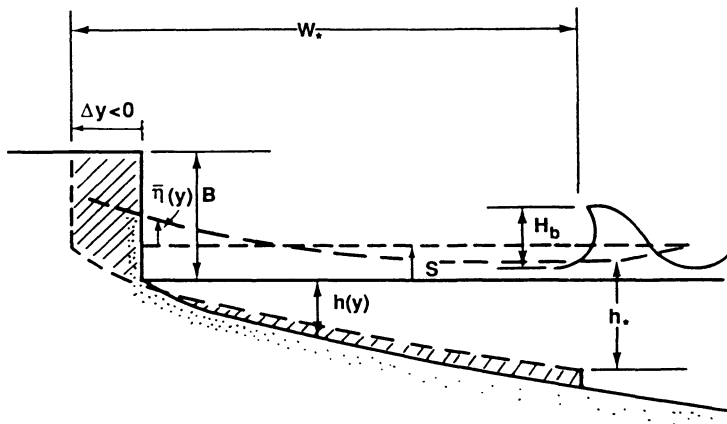Figure 12.   Non-dimensional wave set-up and equilibrium beach profile.

Figure 13. Beach recession due to waves and increased water level, including the effect of wave set-up.

acts to reduce the mean water level over a substantial portion of the surf zone.

For the case in which storm surge is not important and the ratio of breaking wave height to berm height is large, Eq. (26) can be simplified to represent only the effects of waves and wave-induced set-up

$$\frac{\Delta y}{W_*} = -0.053$$

or

$$\Delta y = -0.053 \left(\frac{H_b}{\kappa A}\right)^{3/2} \qquad (28)$$

Thus for a doubled wave height, the recession induced by wave set-up increases by a factor of 2.8.

Profile Adjustment Adjacent to a Seawall Due to Altered Water Level and Waves

We first consider the case of profile lowering adjacent to a seawall due to an elevated water level.

It is well-known that during storms a scour trough will occur adjacent to a sea wall. For purposes here it is appropriate to consider this scour as a profile lowering due to two components: (1) the localized and probably dominant effect due to the interaction of the seawall, waves, and tides, and (2) the effect due to sediment transport offshore to form a profile in

equilibrium with the elevated water level. Applying equilibrium profile concepts, it is possible to calculate only the second component.

The system of interest is presented in Figure 14. The profile is considered to be in equilibrium with virtual origin $y_1 = 0$. For a water level elevated by an amount, S, the equilibrium profile will not be different and will have a virtual origin at $y_2 = 0$. We denote the distances from these virtual origins to the wall as y_{w_1} and y_{w_2} for the original and elevated water levels, respectively. As in previous cases, the approach is to establish the origin, y_{w_2}, (now virtual) such that the sand volumes seaward of the seawall and associated with the equilibrium profiles are equal before and after the increase in water level. In the following, all depths (h values) are referenced to the original water level except h_* which, as described previously, is a reference depth related to the breaking wave height.

Equating volumes as before

$$\int_{y_{W_1}}^{W_*-y_{w_2}+y_{w_1}} h_1(y_1)dy_1 = \int_{y_{w_2}}^{W_2} h_2(y_2)dy_2$$

which can be integrated using $h_1(y) = Ay_1^{2/3}$, and $h_2(y) + S = Ay_2^{2/3}$ and simplified to yield

$$1 - \left[\frac{h'_{w_2}+S'}{h'_*}\right]^{5/2} - \left[1 - \left(\frac{h'_{w_2}+S'}{h'_*}\right)^{3/2}\right]$$
$$+ \left(\frac{1}{h'_*}\right)^{3/2}\right]^{5/3} + \left(\frac{1}{h'_*}\right)^{5/2} \qquad (29)$$
$$- \frac{5}{3}\left(\frac{S'}{h'_*}\right)\left[1 - \left(\frac{h'_{w_2}+S'}{h'_*}\right)^{3/2}\right] = 0$$
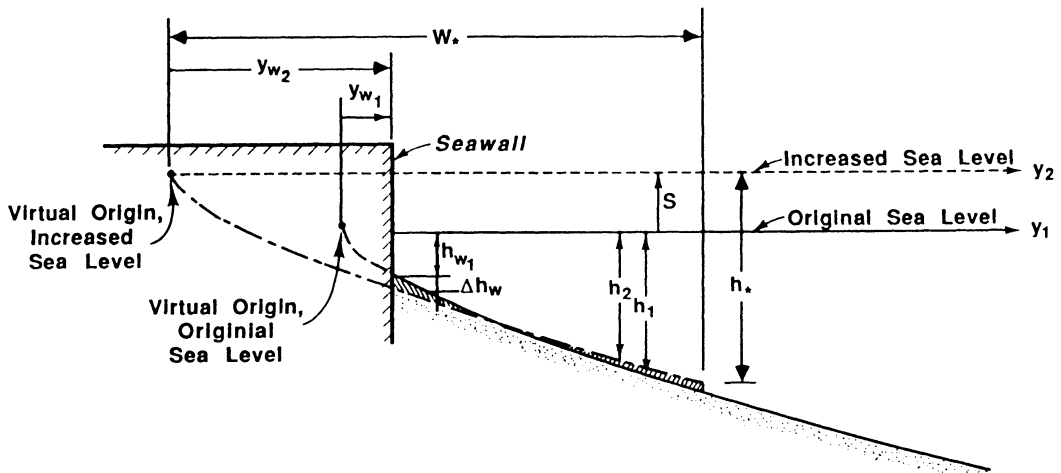
Figure 14. Definition sketch. Profile erosion due to sea level increase and influence of seawall.

in which the primes represent non-dimensional quantities defined as

$$h'_{w_2} = \frac{h_{w_2}}{h_{w_1}}$$

$$h'_* = \frac{h_*}{h_{w_1}} \qquad (30)$$

$$S' = \frac{S}{h_{w_1}}$$

Eq. (29) is implicit in h_{w_2}' and must be solved by iteration. Defining the change in depth at the wall, Δh_w, as

$$\Delta h_w = h_{w_2} - h_{w_1}$$

and in non-dimensional form

$$\Delta h'_w = \frac{\Delta h_w}{h_{w_1}}$$

The quantity $\Delta h_w'$ is now a function of the following two non-dimensional variables: S' and h_*'. The relationship $\Delta h_w'(h_*', S')$ is presented in Figure 15 where it is seen that for a fixed h_*' and increasing S', the non-dimensional scour, $\Delta h_w'$, first increases and then decreases to zero. Figure 16 presents a specific example for $h_*' = 6$. The interpretation of this form is that as S' increases, the profile is no longer in equilibrium and sand is transported seaward to develop the equilibrium profile and the water depth adjacent to the seawall increases. However, as sea

level rises further, with the same total breaking depth, the *active* surf zone width decreases, such that less sand must be transported seaward to satisfy the equilibrium profile. With increasing storm tide, the surf zone width approaches zero at the limit

$$S + h_{w_1} = h_*$$

or

$$S' = h'_* - 1$$

Which corresponds to the upper line in Figure 15. It is emphasized that the increased depth at the seawall predicted here does not include the scour interaction effect of the seawall and waves.

We next consider the case of lowered water level ($S < 0$) adjacent to a seawall as shown in Figure 17. In this case sediment will move landward due to the disequilibrium caused by the lowered water level. The notation is the same as in the previous case. Equating volumes eroded and deposited is expressed as

$$\int_{y_{w_1}}^{W_A - y_{w_2} + y_{w_1}} h_1(y) dy_1$$

$$= \int_{y_{w_2}}^{W_*} h_2(y_2) dy_2 + h_*(W' - W_*) \qquad (31)$$

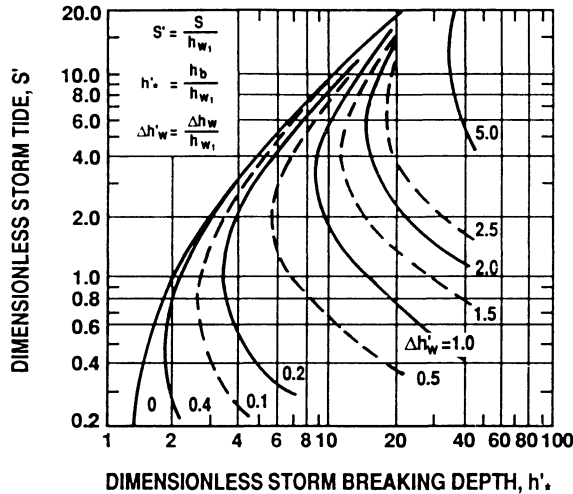which can be integrated and simplified to yield

Figure 15.   Isolines of dimensionless seawall toe scour, $\Delta h'_W$ vs dimensionless storm tide, S' and dimensionless breaking depth h'_*.
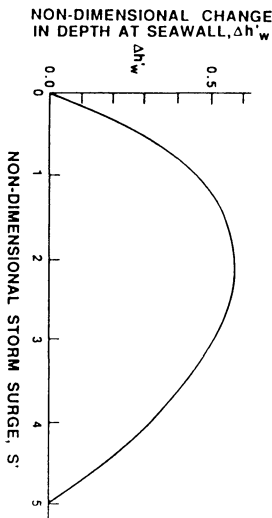

Figure 16.   Non-dimensional change in water depth at wall $\Delta h'_W$ as a function of non-dimensional breaking depth $h'_* = 6.0$.

$$(h'_{W_2}+S')^{3/2}\left[\frac{3}{5}(h'_{W_2}+S')-h'_*\right] - \frac{2}{5}(h'_*-S')^{5/2}$$
$$+ \left(h'_*-S'-\frac{3}{5}\right) + \frac{2}{5}h'^{5/2}_* = 0 \qquad (32)$$

The non-dimensional distance W'_A ($\equiv W_A/W_*$) is given by

$$W'_A = \left(1 - \frac{S'}{h'_*}\right)^{3/2} + y'_{W_2} - y'_{W_1} \qquad (33)$$

The non-dimensional depth change (decrease) at the wall is

$$\Delta h'_W = h'_{W_2} - 1 \qquad (34)$$

which can be established by solving Eq. (32). Figure 18 presents a plot of $\Delta h'_W(h'_*, S')$.

In Eq. (32), the term $h'_{W_2} + S'$ represents the non-dimensional total depth at the seawall on the equilibrium profile for the lowered water level. A limiting case for the above formulation is for this water depth to be zero, i.e. $h'_{W_2} + S' = 0$, yielding

$$-\frac{2}{5}(h'_*-S')^{5/2}+\left(h'_*-S'-\frac{3}{5}\right)+\frac{2}{5}h'^{5/2}_* = 0 \qquad (35)$$

which is plotted as the upper dashed line in Figure 18.

Response from Initial Uniform Slope

For simplicity, many wave tank tests commence with an initially planar beach slope, m_i. It is of interest to examine the relationship of the equilibrium and initial profiles. As presented in Figure 19, there are five types of equilibrium profiles that can form depending on the initial slope, m_i, and the sediment and wave
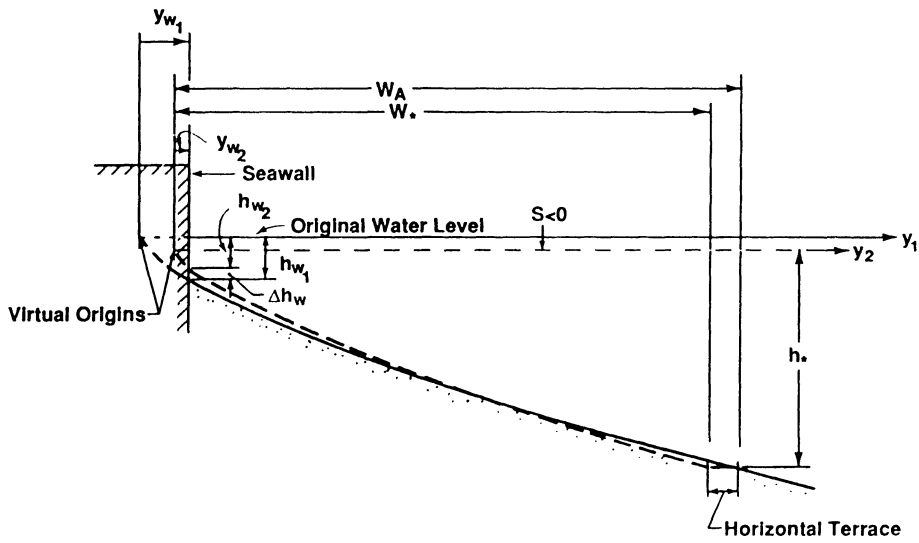
Figure 17.   Definition sketch, profile response adjacent to a seawall for case of lowered sea level.
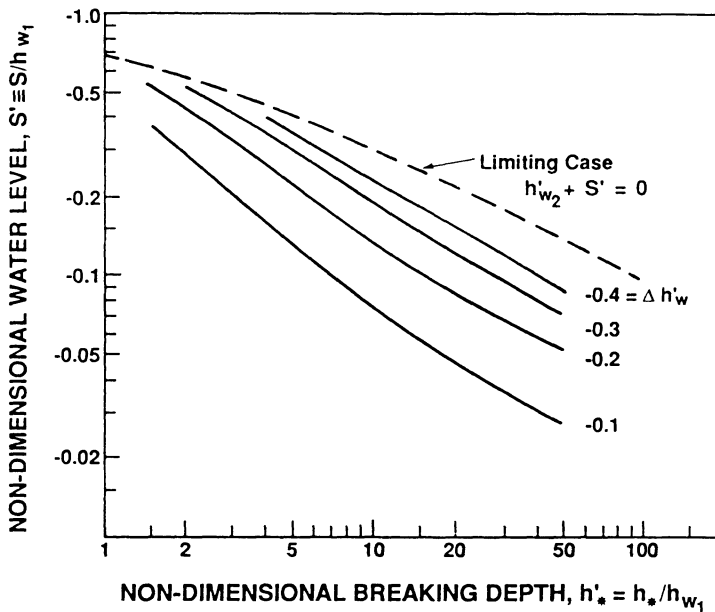

Figure 18.   Non-dimensional shallowing adjacent to a seawall due to lowering of water level. Variation with non-dimensional breaking depth, h'_* and non-dimensional water level, S'.
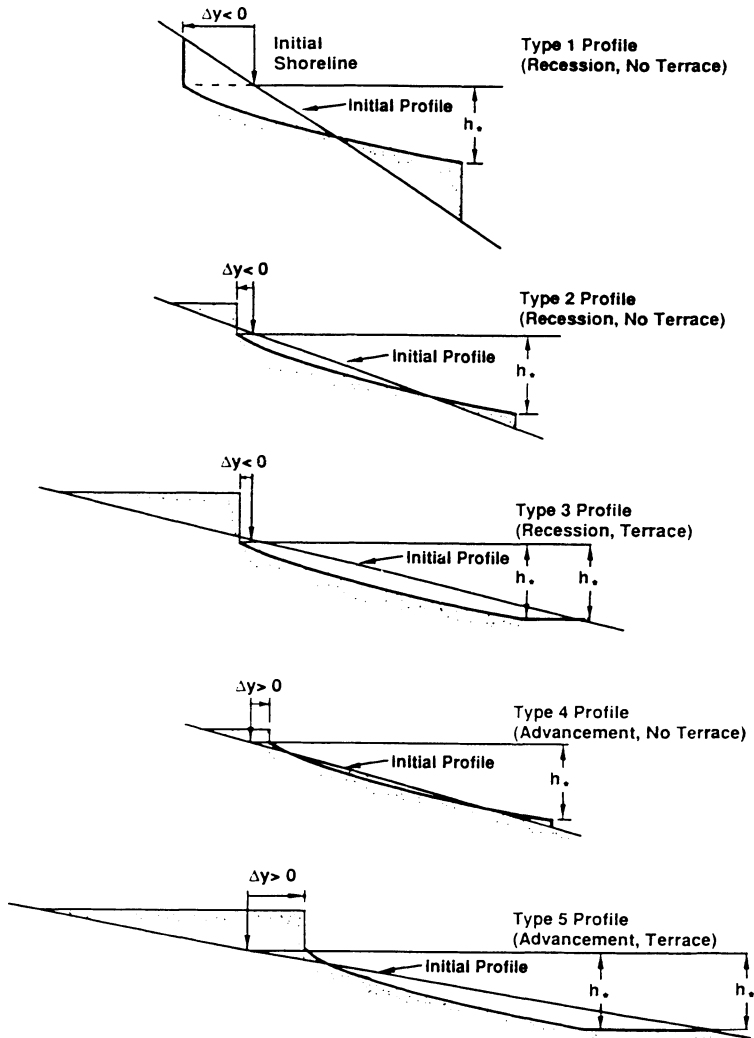
Figure 19.   Illustration of five equilibrium profile types commencing from an initially uniform slope.

characteristics. Wave tank tests by SUNA-MURA and HORIKAWA (1974) identified profile Types 1, 2 and 5. Shoreline responses for Types 1 and 3 have been investigated by SUH and DALRYMPLE (1988) using equilibrium profile concepts and good agreement with wave tank data was demonstrated.

Referring to Figure 19, for the Type 1 profile the initial slope is much steeper than that for the equilibrium profile and only seaward sediment transport occurs. An additional charac-

teristic is that a scarp is formed at the shoreline and no berm is deposited. The wave tank profile presented in Figure 5 is an example of a Type 1 profile. Type 2 profile, also a case of shoreline recession, occurs for a somewhat milder relative slope (initial to equilibrium), sediment transport occurs in both the onshore and offshore directions and a berm is formed at the shoreline. With still milder relative slopes, sediment transport occurs only shoreward resulting in a Type 3 profile characterized by shore-

line recession with all of the sediment transported deposited as a berm feature. A terrace or "bench" (here assumed horizontal) is formed at the seaward end of the equilibrium profile. This type profile is probably the least likely to occur due to the unrealistically high berm elevation required. Type 4 profile is one of shoreline advancement, occurring for still milder initial slopes and is characterized by sediment transport in both the landward and seaward directions. Finally, Type 5 profile is one of shoreline advancement with only landward sediment transport and leaving a horizontal terrace or bench at the seaward end of the equilibrium profile. The following paragraphs quantify the profile characteristics and shoreline changes for each of these five types. As described previously, shoreline recession and advancement will be denoted by negative and positive Δy, respectively. It will be shown that the non-dimensional shoreline change, $\Delta y' (\equiv \Delta y/W_*)$ is a function of the non-dimensional depth of limiting profile change, $h'_* (\equiv h_*/W_* m_i)$ and non-dimensional berm height, $B' (\equiv B/W_* m_i)$. The developments associated with these profile types will not be presented in detail. Methods are similar to those applied earlier in this report for example for the case of shoreline recession due to an elevated water level. Figure 20 presents $\Delta y'(h'_*, B')$ and the associated regions of occurrence for the five profiles types.

Type 1 Profile

The non-dimensional advancement, $\Delta y'$, can be expressed in terms of the non-dimensional depth of limiting motion, h'_*, as

$$\Delta y' = \frac{3}{5}h'_* - \frac{1}{2} \qquad (36)$$

where for this profile type, $\Delta y' < 0$. Because no berm is formed, the berm characteristics do not appear in this expression and B is simply a reference quantity when plotted in Figure 20.

It can be shown that the non-dimensional volume, V', transported seaward past any location, y', is

$$V' \equiv \frac{V}{BW_*} = -\frac{1}{2B'}[y'^2 - (\Delta y')^2] + \frac{3h'_*}{5B'}(y' - \Delta y')^{5/3}, \quad \Delta y' < y' < 1 + \Delta y' \qquad (37)$$

in which

$$y' \equiv \frac{y}{W_*} \qquad (38)$$

For this type profile, SUH and DALRYMPLE (1988) have denoted h_*/W_* as the equilibrium slope, m_e, and have shown a correlation between the ratio of initial to equilibrium slopes and the resulting profile changes.

Type 2 and Type 4 Profiles

For these profile types, the non-dimensional change, $\Delta y'$, depends on h'_* and non-dimensional berm height, B',

$$\Delta y' = -(B'+1) + \sqrt{2B' + \frac{6}{5}h'_*}. \qquad (39)$$

For type 2 and Type 4 profiles, the values of $\Delta y'$ will be negative (recession) and positive (advancement), respectively.

The equations for non-dimensional volumes transported seaward past any location, y', for Type 2 and Type 4 profiles are

$$V' = \frac{1}{2B'}[B'^2 - y'^2] \\ - (y' + B'), \quad -B' < y' < \Delta y' \qquad (40a)$$

$$V' = -(\Delta y' + B') - \frac{1}{2B'}(y'^2 - B'^2) + \frac{3h'_*}{5B'} \\ (y' - \Delta y')^{5/3}, \quad \Delta y' < y' < 1 + \Delta y' \qquad (40b)$$

Type 3 and Type 5 Profiles

Both of these equilibrium profile types include a horizontal terrace at their seaward limits. The expressions for $\Delta y'$ are identical:

$$\Delta y' = \frac{1}{2} \frac{h'^2_* - B'^2 - \frac{4}{5}h'_*}{h'_* + B'} \qquad (41)$$

where again $\Delta y'$ is negative and positive for profile Types 3 and 5, respectively.

The equations for non-dimensional volumes transported seaward past any location, y', for Type 3 and Type 5 profiles are
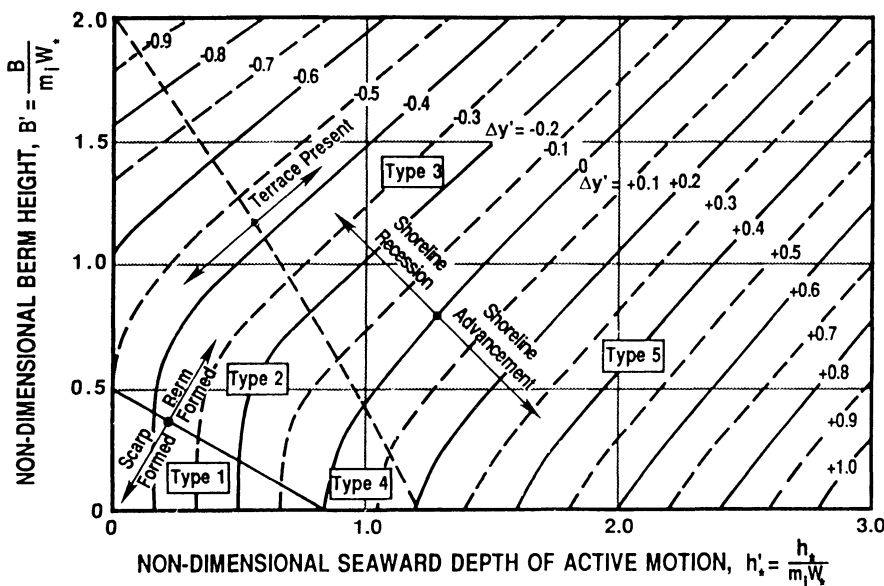
Figure 20. Regimes of equilibrium profile types commencing from an initially planar profile showing five types of equilibrium profiles and non-dimensional profile advancement, $\Delta y'$.

$$V' = \frac{1}{2B'}(B'^2 - y'^2) \quad (42a)$$
$$- (y' + B') , \quad -B' < y' < \Delta y'$$

$$V' = -\frac{1}{2B'}(y'^2 - B'^2) + \frac{3h'_*}{5B'}(y' \quad (42b)$$
$$- \Delta y')^{5/3} - (\Delta y' + B') , \quad \Delta y' < y' < 1 + \Delta y'$$

$$V' = -\frac{2h'_*}{5B'} - \Delta y'\left(1 + \frac{h'_*}{B'}\right) - \frac{B'}{2} \quad (42c)$$
$$-\frac{1}{2B'}y'^2 + \frac{h'_*}{B'}y' , \quad 1 + \Delta y' < y' < h'_*.$$

Limits of Profiles Types

The criterion for berm formation is

$$B' + \frac{3}{5}h'_* - \frac{1}{2} \begin{cases} < 0, \text{ No Berm Formed} \\ > 0, \text{ Berm Formed} \end{cases} \quad (43)$$

Here B' is interpreted as the non-dimensional berm height that would be formed if the berm height exceeds the scarp height cut by the shoreline recession into the uniform slope profile. For berm formation, $\Delta y > -B/m_i$.

The limit for terrace formation is

$$(B' + h'_*)^2 - 2B' - \frac{6}{5}h'_* \begin{cases} < 0, \text{ No Terrace} \\ > 0, \text{ Terrace} \end{cases} \quad (44)$$

The limit for no shoreline change, $\Delta y' \equiv 0$, depends on whether or not a terrace is present.

No Terrace Present

$$B'^2 - \frac{6}{5}h'_* + 1 \begin{cases} = 0, \text{ No Shoreline Change} \\ > 0, \text{ Shoreline Recession} \\ < 0, \text{ Shoreline Advancement} \end{cases} \quad (45)$$

Terrace Present

$$B'^2 - h'_*{}^2 + \frac{4}{5}h'_* \begin{cases} = 0, \text{ No Shoreline Change} \\ > 0, \text{ Shoreline Recession} \\ < 0, \text{ Shoreline Advancement} \end{cases} \quad (46)$$

Figures 21 and 22 present examples of profile response and associated volumes transported for profile Types 1 and 4.

Perched Beach

The offshore extent of a perched beach is terminated by a shore parallel structure which prevents the sand from moving seaward. In conjunction with a beach nourishment project, it is pos-
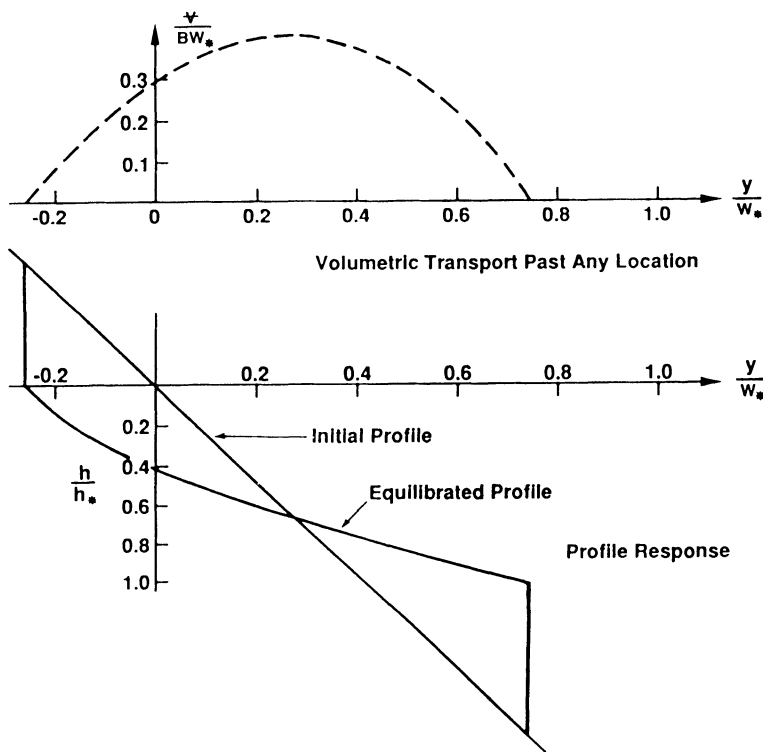
Figure 21.   Example of Type 1 (recession) profile response from an initially uniform slope and associated volumetric transport. Note only positive (seaward) transport.

sible in principle to obtain a much wider beach for the same volume of added sediment. Denoting the "native" and "fill" sediment scale parameters as A_N and A_F respectively (c.f. Eq. (3)). Referring to Figure 23 for terminology, the required volume, V, for the case of the sand just even with the top of the submerged breakwater is

$$V = B\left[\left(\frac{h_1}{A_N}\right)^{3/2} - \left(\frac{h_2}{A_F}\right)^{3/2}\right] \\ + \frac{3}{5}\left[A_N\left(\frac{h_1}{A_N}\right)^{5/2} - A_F\left(\frac{h_2}{A_F}\right)^{5/2}\right] \tag{47}$$

and the added beach width, Δy, is

$$\Delta y = \left(\frac{h_1}{A_N}\right)^{3/2} - \left(\frac{h_2}{A_F}\right)^{3/2} \tag{48}$$

Referring to Figure 23, it is possible to calculate the reduction in required volume through a perched beach design. The results can be developed for intersecting and non-intersecting type profiles (c.f. Figure 24a and b). For simplicity, only the results for non-intersecting profiles (without the sill) will be presented here. The fractional reduction in volume, $\frac{\Delta V}{V_1}$, is given by

$$\frac{\Delta V}{V_1} = 1 - \frac{\Delta y' + \frac{3}{5B'}\left[(h'_1)^{5/2} - \left(\frac{A_N}{A_F}\right)^{3/2}(h'_2)^{5/2}\right]}{\Delta y' + \frac{3}{5B'}\left\{\left[\Delta y' + \left(\frac{A_N}{A_F}\right)^{3/2}\right]^{5/3} - \left(\frac{A_N}{A_F}\right)^{3/2}\right\}} \tag{49}$$

in which V_1 = the volume that would be required to advance the shoreline seaward by an amount, Δy, without the sill and $y'_2 = y_2/W_*$, $h'_1 = h_1/h_*$, $h'_2 = h_2/h_*$, $\Delta y' = \Delta y/W_*$, and $B' = B/h_*$.

As an example of the application of Eq. (49), consider the following parameters: $A_N = A_F = 0.15$ m$^{1/3}$, $h_* = 6$ m, $h_1 = 4$ m, $h_2 = 3$ m, $B = 2.0$ m, and $\Delta y = 48.3$ m (From Eq. (48)).
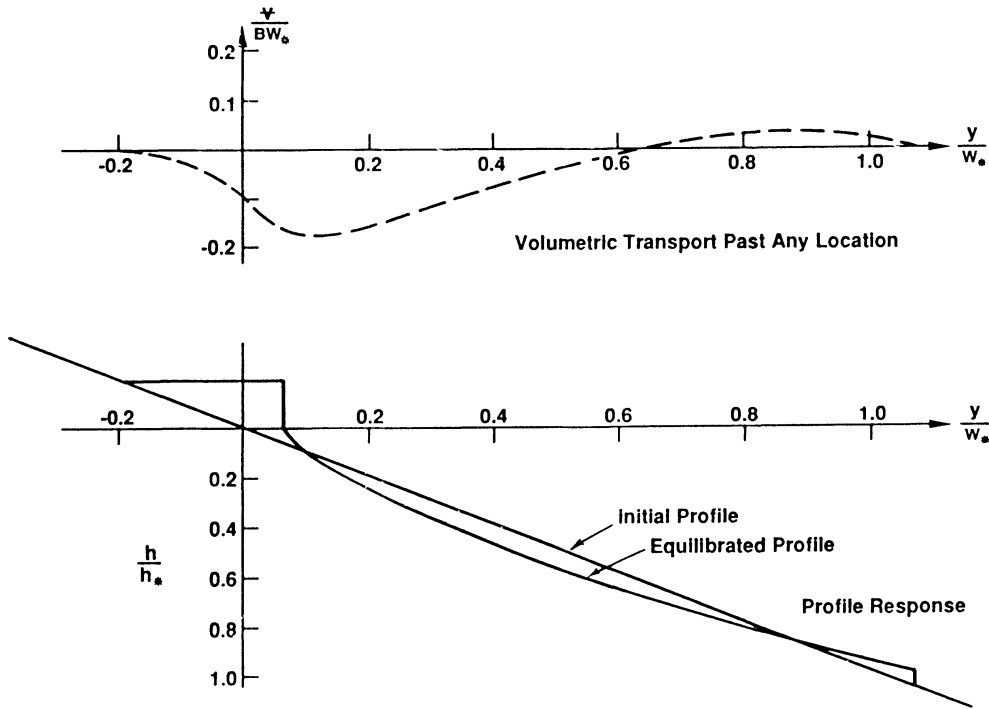
Figure 22. Example of Type 4 (advanced) profile response from an initially uniform slope and associated volumetric transport. Note both positive (seaward) and negative (landward) transport.
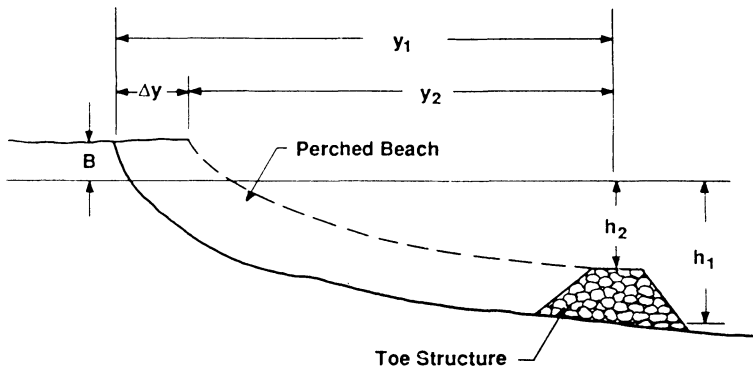
Figure 23. Perched beach, demonstration of nourishment volumes saved.

The width of the surf zone without the sill, W_*, is $W_* = (h_*/A_N)^{3/2} = 253.0$ m and $y_2 = (h_2/A_F)^{3/2} = 89.4$ m.

The fractional reduction in volume is $\Delta V/V_1 = 0.342$ i.e., there is a 34% reduction in sand volumes with the perched beach design.

Profile Response to Beach Nourishment

Intersecting, Non-Intersecting and Submerged Profiles.
Beach nourishment is considered with sediment of arbitrary but uni-

Figure 24.   Three Generic Types of Nourished Profiles. (a) Intersecting Profile, (b) Non-Intersecting Profile, and (c) Submerged Profile.
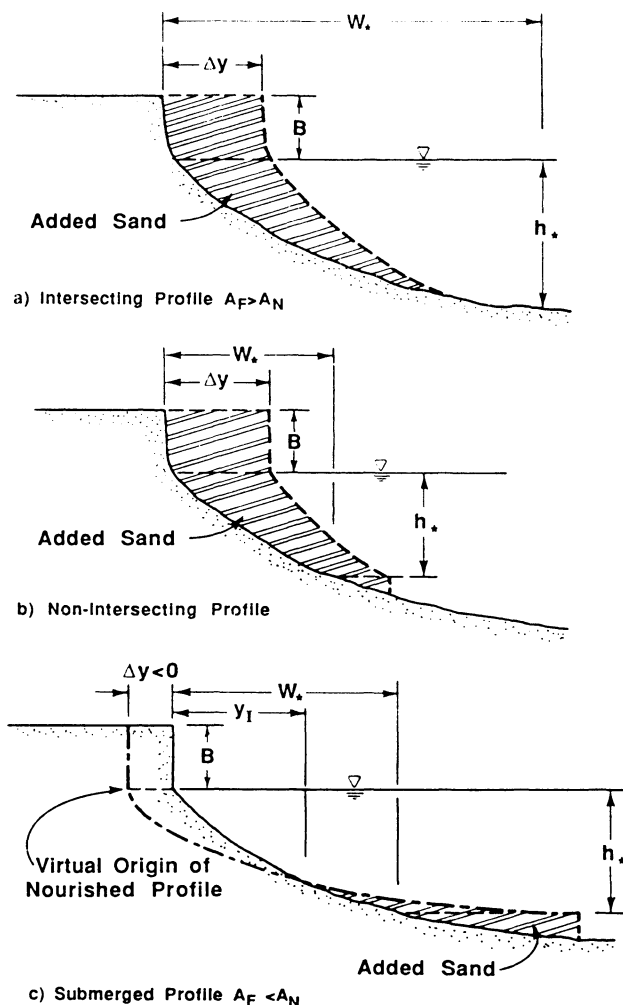
form diameter. As indicated in Figure 24, nourished beach profiles can be designated as "intersecting," "non-intersecting," and "submerged" profiles. A necessary but insufficient requirement for profiles to intersect is that the placed material be coarser than the native. Similarly, non-intersecting or submerged profiles will always occur if the placed sediment is the same size as or finer than the native. However, non-intersecting profiles can occur if the placed sediment is coarser than the native. For "submerged" profiles to occur, the placed material

must be finer than the native. Figure 25 illustrates the effect of placing the same volume of four different sized sands. In Figure 25a, sand coarser than the native is used, intersecting profiles result and a relatively wide beach Δy is obtained. In Figure 25b, the same volume of sand of the same size as the native is used, non-intersecting profiles result and the dry beach width gained is less. More of the same volume is required to fill out the milder sloped underwater profile. In Figure 25c, the placed sand is finer than the native and much of the sand is
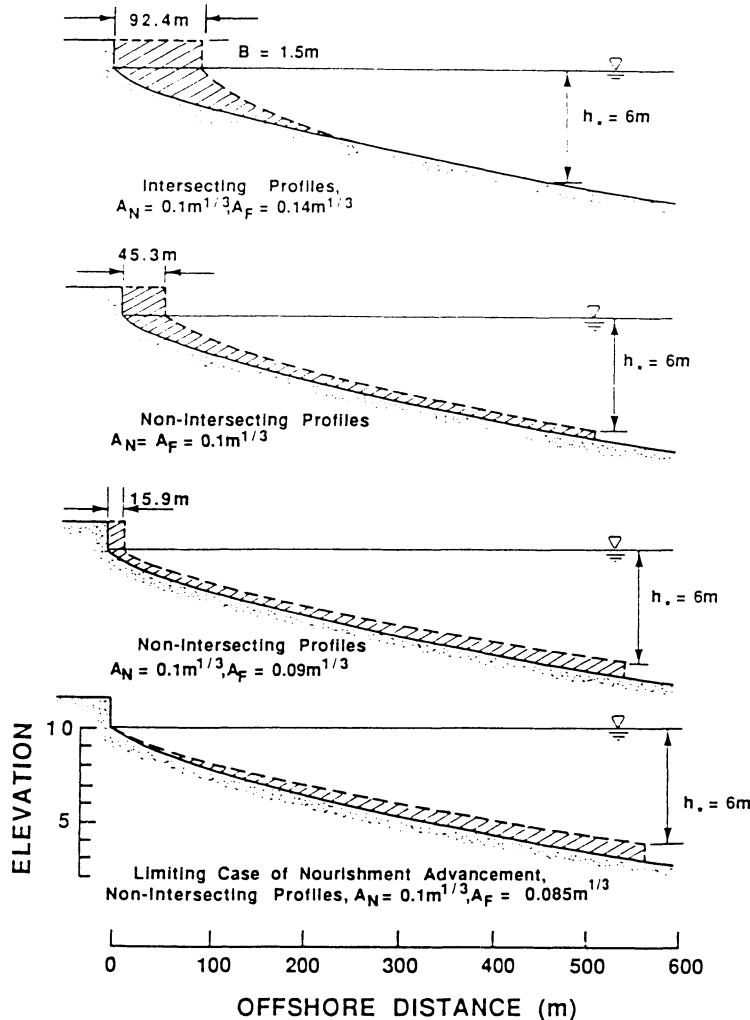
Figure 25.   Effect of nourishment material scale parameter, A_F, on width of resulting dry beach. Four examples of decreasing A_F with same added volume per unit beach length.

used in satisfying the milder sloped underwater profile requirements. In a limiting case, shown in Figure 25d, no dry beach is yielded with all the sand being used to satisfy the underwater requirements. Figures 26a through 26d illustrate the effects of nourishing with greater and greater quantities of a sand which is considerably finer than the native. Figure 26d is the case of formation of an incipient dry beach, i.e. the same as in Figure 25d. With increasing volumes, the landward intersection of the native and placed profiles occurs closer to shore and

the seaward limit of the placed profile moves seaward.

We can quantify the results presented in Figures 24, 25 and 26 by utilizing equilibrium profile concepts. It is necessary to distinguish the three cases noted in Figure 24. The first is with intersecting profiles such as indicated in Figure 24a and requires $A_F > A_N$. For this case, the volume placed per unit shoreline length, V_1 associated with a shoreline advancement, Δy, is presented in non-dimensional form as
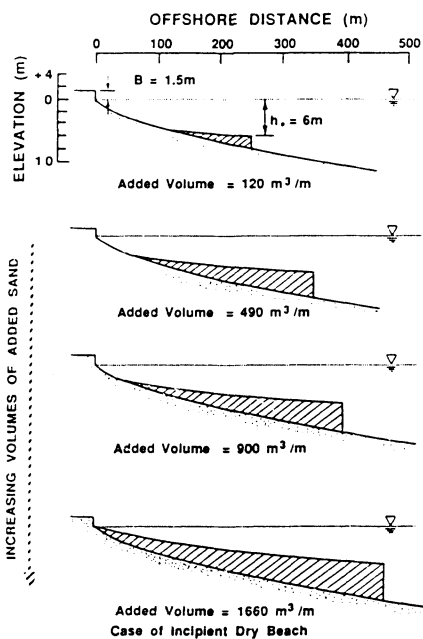
Figure 26. Effect of increasing volume of sand added on resulting beach profile. A_F = 0.1 m$^{1/3}$, A_N = 0.2 m$^{1/3}$, h = 6 m, B = 1.5 m.

$$V'_1 = \Delta y' + \frac{3}{5B'}(\Delta y')^{5/3}\frac{1}{\left[1 - \left(\dfrac{A_N}{A_F}\right)^{3/2}\right]^{2/3}} \quad (50)$$

in which $V'_1 (\equiv V_1/BW_*)$ is the non-dimensional volume, B is the berm height, W_* is a reference offshore distance associated with the breaking depth, h_*, on the original (unnourished) profile, *i.e.*

$$W_* = \left(\frac{h_*}{A_N}\right)^{3/2} \quad (51)$$

and the breaking depth, h_* and breaking wave height, H_b are related by $h_* = H_b/\kappa$ with $\kappa(\approx 0.78)$, the spilling breaking wave proportionality factor.

For non-intersecting but emergent profiles (Figure 24b), the corresponding volume V_2 in non-dimensional form is

$$V'_2 = \Delta y' + \frac{3}{5B'} \quad (52)$$
$$\left\{\left[\Delta y' + \left(\frac{A_N}{A_F}\right)^{3/2}\right]^{5/3} - \left(\frac{A_N}{A_F}\right)^{3/2}\right\}$$

It can be shown that the critical value of $(\Delta y')$ for intersection/non-intersection of profiles is given by

$$\Delta y' + \left(\frac{A_N}{A_F}\right)^{3/2}$$
$$- 1 \begin{cases} < 0, \text{ Intersecting Profiles} \\ > 0, \text{ Non-Intersecting Profiles} \end{cases} \quad (53)$$

The critical *volume* associated with intersecting/non-intersecting profiles is

$$(V')_{c1} = \left(1 + \frac{3}{5B'}\right)\left[1 - \left(\frac{A_N}{A_F}\right)^{3/2}\right] \quad (54)$$

and applies only for $(A_F/A_N) > 1$. Also of interest, the critical volume of sand that will just yield a finite shoreline displacement for non-intersecting profiles $(A_F/A_N < 1)$, is

$$(V')_{c2} = \frac{3}{5B'}\left(\frac{A_N}{A_F}\right)^{3/2}\left(\frac{A_N}{A_F} - 1\right) \quad (55)$$

Figure 27 presents these two critical volumes versus the scale parameter ratio A_F/A_N for the special case $h_*/B = 4.0$, i.e. $B' = 0.25$.

The results from Eqs. (50), (52) and (53) are presented in graphical form in Figures 28 and 29 for cases of $(h_*/B) = 2$ and 4. Plotted is the non-dimensional shoreline advancement $(\Delta y')$ versus the ratio of fill to native sediment scale parameters, A_F/A_N, for various isolines of dimensionless fill volume $V'\left(= \dfrac{V}{W_*B}\right)$ per unit length of beach. It is interesting that the shoreline advancement increases only slightly for $A_F/A_N > 1.2$; for smaller values the additional shoreline width, Δy, decreases rapidly. For A_F/A_N values slightly smaller than plotted, there is no shoreline advancement, i.e. as in Figure 25d.

Referring to Figure 24c for submerged profiles, it can be shown that

$$\frac{\Delta y}{y_I} = 1 - \left(\frac{A_N}{A_F}\right)^{3/2} \quad (56)$$

where $\Delta y < 0$ and the non-dimensional volume of added sediment can be expressed as

$$V' = \frac{3}{5B'}\left\{\left[\left(\frac{A_N}{A_F}\right)^{3/2} + \Delta y'\right]^{5/3}\right.$$
$$\left. - \frac{(-\Delta y')^{5/3}}{\left[\left(\dfrac{A_N}{A_F}\right)^{3/2} - 1\right]^{2/3}} - \left(\frac{A_N}{A_F}\right)^{3/2}\right\} \quad (57)$$
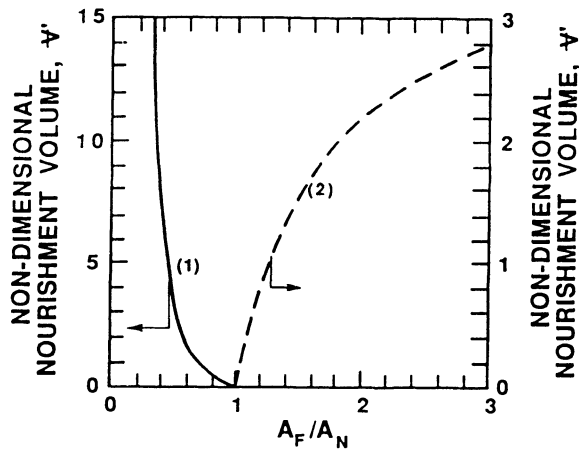
Figure 27. (1) Volumetric requirement for finite shoreline advancement (Eq. 55); (2) Volumetric criterion for intersecting profiles (Eq. 54). Variation with A_F/A_N. Results presented for $h_*/B = 4.0$.

Variation in Sediment Size Across the Surf Zone

All cases presented earlier have considered the sand size to be of uniform size across the surf zone. In most cases, there is some sorting with the sand grading to finer sizes in the seaward direction. With the relation of $A(D)$, and thus $\mathscr{D}_*(D)$, known (c.f. Eq. (5)) it is possible to calculate equilibrium profiles for cases of a continuous variation of sand sizes across the surf zone and a distribution composed of piecewise uniform diameter segments.

Continuous Arbitrary Distribution of Sand Sizes Across the Surf Zone. The differential equation for an equilibrium beach profile is given by

$$\frac{\partial h^{3/2}}{\partial y} = A^{3/2}(D) \qquad (58)$$

from which Eq. (1) is obtained readily. Integrating across the surf zone yields the equilibrium profile

$$h^{3/2}(y) = \int_0^y A^{3/2}(D)dy \qquad (59)$$

If the sediment scale parameter, A, varies linearly with distance offshore, y, it is possible to develop an analytical solution of Eq. (58). Figure 30 presents a comparison of equilibrium profiles for uniform and linearly varying A val-

ues. The two uniform cases are for A equal to 0.1 m$^{1/3}$ and 0.068 m$^{1/3}$ corresponding to sediment diameters of 0.2 mm and 0.1 mm, respectively (Figure 1). The profiles for these two cases are presented as the dashed lines in Figure 30b. As presented in Figure 30a, for the remaining case, the A value varies linearly from 0.1 m$^{1/3}$ to 0.068 m$^{1/3}$ at 800 meters seaward, in accordance with a decreasing sediment size with distance offshore. The profile for this case is the solid line in Figure 30b. As expected: (1) the two profiles for $A = 0.1$ m$^{1/3}$ and variable A agree in shallow water since they differ little in this region, and (2) the profile for varying A lies between the two profiles associated with the limiting A values for the variable A profile.

Piecewise Uniform Sand Sizes Across the Surf Zone. Denoting the sand size as D_n over the segment $y_n < y < y_{n+1}$, the water depth in this region is obtained from a slight variation of Eq. (59)

$$h^{3/2}(y) = h^{3/2}(y_n) + A^{3/2}(D_n)[y - y_n] \qquad (60)$$

which applies for $y_n < y < y_{n+1}$.

Comparison with Empirical Orthogonal Functions

It is instructive to compare results obtained from a simple application of the equilibrium beach profile with those developed by various
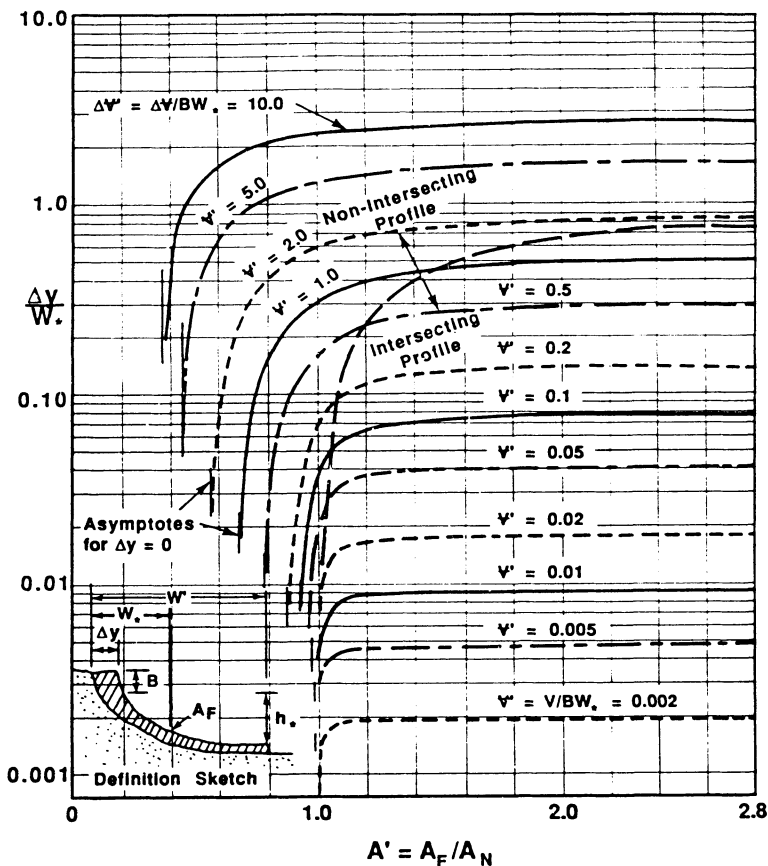
Figure 28. Variation of non-dimensional shoreline advancement $\Delta y/W_*$, with A' and $\mathcal{V}$. Results shown for $h_*/B = 2.0$.

researchers (*e.g.* WINANT, INMAN and NORDSTROM (1975) and WEISHAR and WOOD (1983)) in their application of Empirical Orthogonal Function (EOF) methods to time series of natural beach profiles. This method has been described by HAYDEN *et al.* (1975). For purposes here, we note that the first EOF is analogous to the equilibrium beach profile and the second EOF is termed the "berm-bar" function.

We will consider the change in profile elevation resulting from a *single* elevated water level and wave and sediment conditions that would mobilize sediment out to a depth h_*. Consideration of Figure 8 and utilizing Eq. (13), the first EOF is the average profile, and the second EOF is obtained by balancing eroded and accreted

volumes and can be shown to be approximately

$$\frac{\Delta h}{h_*} = \Delta h'$$

$$= \begin{cases} B'(1-S') + (y' - \Delta y')^{2/3} & , \Delta y' < y' < 0 \\ (y' - \Delta y')^{2/3} - y'^{2/3} - S'B' & 0 < y' < 1 + \Delta y' \end{cases}$$

(61)

and where the primed (non-dimensional) quantities are as defined by Eqs. (14). Figure 31 presents a comparison between Eq. (61) and the second EOF as determined by WINANT *et al.* (1975) based on field measurements at Torrey Pines, California. The similarities between the EOF obtained by these investigators and those developed by equilibrium profile synthesis are evident.
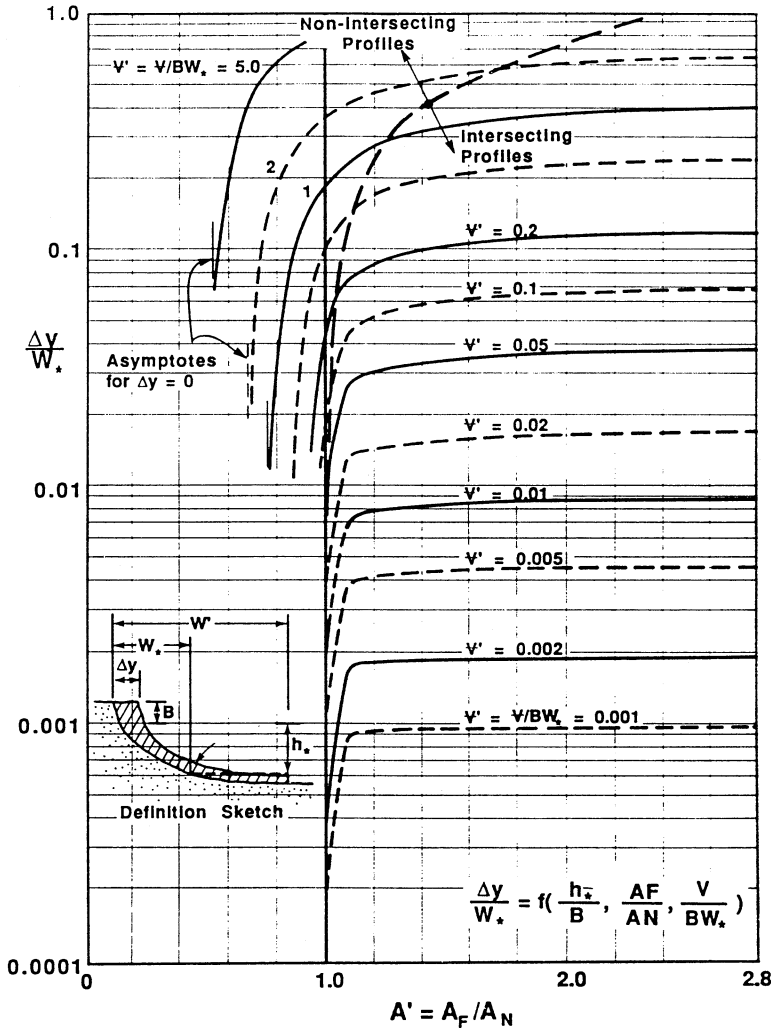
Figure 29.   Variation of non-dimensional shoreline advancement $\Delta y/W_*$, with A' and V. Results shown for $h_*/B = 4.0$.

Effects of Sea Level Rise on Beach Nourishment Quantities

Recently developed future sea level scenarios (HOFFMAN *et al.*, 1983) have been developed based on assumed fossil fuel consumption and other relevant factors and have led to concern over the viability of the beach nourishment option for erosion control. First, in the interest of objectivity, it must be stated that the most extreme of the scenarios published by the Environmental Protection Agency (EPA) amounting to sea level increases exceeding 3.4 m by the

year 2100 are extremely unlikely. While it is clear that worldwide sea level has been rising over the past century and that the rate is likely to increase, the future rate is very poorly known. Moreover, probably at least 20 to 40 years will be required before our confidence level of future sea level rise rates will improve substantially. Within this period, it will be necessary to assess the viability of beach restoration on a project-by-project basis in recognition of possible future sea level scenarios. Presented below is a basis for estimating nourishment needs for the scenarios in which there is no
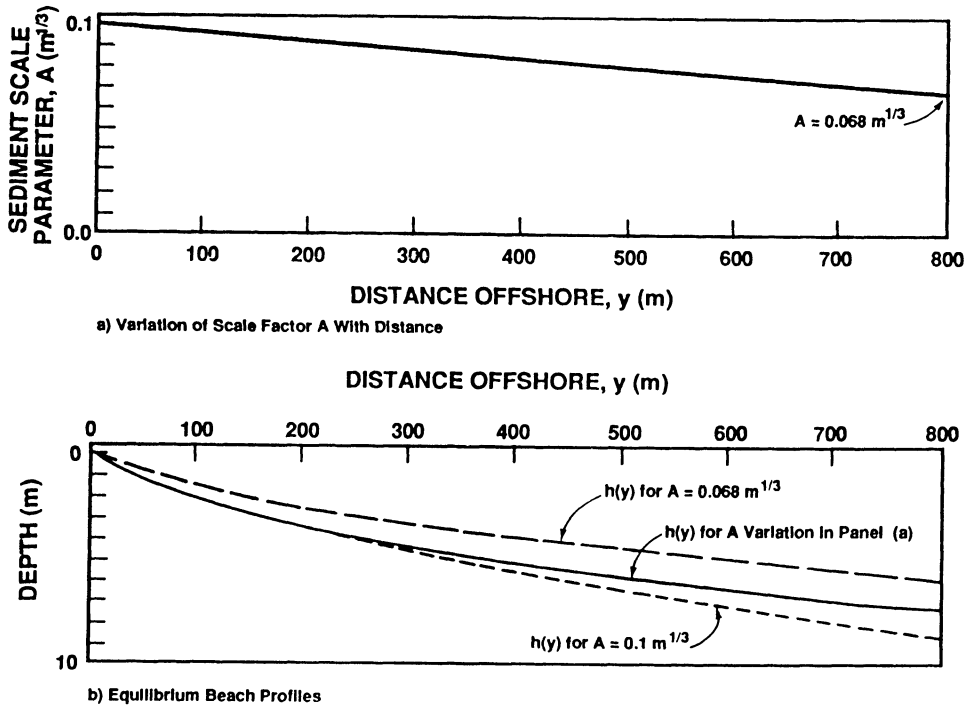
Figure 30. Example comparing equilibrium beach profiles for uniform sediment scale parameters (two dashed curves, panel b) and linearly varying sediment scale parameter shown in panel a (associated profile is solid curve, panel b).

landward sediment transport across the continental shelf and there is a more-or-less well-defined seaward limit of sediment motion; in the second case the possibility of onshore sediment transport will be discussed.

Case I—Nourishment Quantities for the Case of No Onshore Sediment Transport.

The Bruun Rule (1962) is based on the consideration that there is a well-defined depth limit, h_*, of sediment transport. With this assumption, the only response possible to sea level rise is seaward sediment transport. Considering the total shoreline change Δy, to be the superposition of recession due to sea level rise Δy_S and the advancement due to beach nourishment, Δy_N,

$$\Delta y = \Delta y_S + \Delta y_N \qquad (62)$$

and, from the Bruun Rule (Eq. 15)

$$\Delta y_S = -S\frac{W_*}{h_*+B} \qquad (63)$$

in which S is the sea level rise, W_* is the dis-

tance from the shoreline to the depth, h_*, associated with the seaward limit of sediment motion and B is the berm height. Assuming that compatible sand is used for nourishment (i.e. $A_F = A_N$)

$$\Delta y_N = \frac{V}{h_* + B} \qquad (64)$$

and V is the beach nourishment volume per unit length of beach. Therefore

$$\Delta y = \frac{1}{(h_*+B)}[V - SW_*] \qquad (65)$$

The above equation can be expressed in rates by,

$$\frac{dy}{dt} = \frac{1}{(h_*+B)}\left[\frac{dV}{dt} - W_*\frac{dS}{dt}\right] \qquad (66)$$

were dS/dt now represents the rate of sea level rise and dV/dt is the rate at which nourishment material is provided. It is seen from Eq. (66) that in order to maintain the shoreline stable due to the effect of sea level rise the nourish-
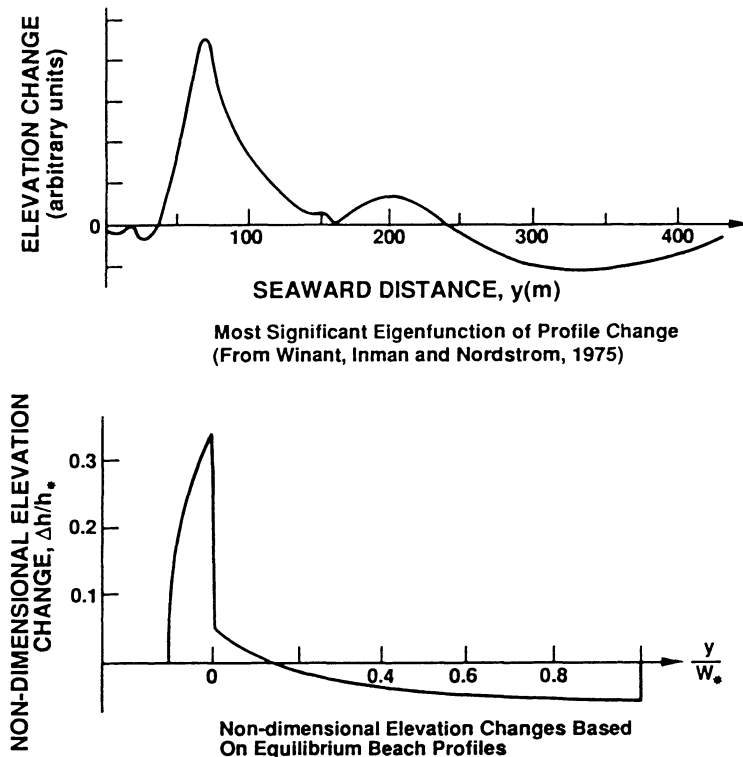
Figure 31. Comparison of beach profile elevation changes by equilibrium profile concepts with results from field measurements.

ment rate dV/dt is related to the rate of sea level rise dS/dt by

$$\frac{dV}{dt} = W_* \frac{dS}{dt} \qquad (67)$$

Of course, this equation applies only to cross-shore mechanisms and therefore does not recognize any other causes of background erosion or longshore transport losses from the project area. It is seen that W_* behaves as an amplifier of material required. Therefore, it is instructive to examine the nature of W_* and it will be useful for this purpose to consider the equilibrium profile given by Eq. (1),

$$W_* = \left(\frac{H_b}{\kappa A}\right)^{3/2} \qquad (68)$$

i.e. W_* increases with breaking wave height and with decreasing A (or sediment size).

Case II—Nourishment Quantities for the Case of Onshore Sediment Transport.

Evidence is accumulating that in some locations there is a substantial amount of onshore sediment transport across the continental shelf. DEAN (1987b) has noted the consequences of the assumption of a "depth of limiting motion" in allowing only offshore transport as a response to sea level rise and proposed instead that if this assumption is relaxed, onshore transport can occur leading to a significantly different profile response to sea level rise. Consider that there is a range of sediment sizes in the active profile with the hypothesis that a sediment particle of given hydraulic characteristics is in equilibrium under certain wave conditions and at a particular water depth. Thus, if sea level rises our reference particle will seek equilibrium which requires *landward* rather than seaward transport as required by the

Bruun Rule. Figure 32 summarizes some of the elements of this hypothesis.

Turning now to nourishment requirements in the presence of onshore sediment transport, the conservation of sediment yields

$$\frac{\partial Q}{\partial y} = \frac{\partial h}{\partial t} + \text{sources} - \text{sinks} \qquad (69)$$

in which h is the water depth referenced to a *fixed* vertical datum and the sources could include natural contributions such as hydrogenous or biogenous components, and suspended deposition or human related contributions, *i.e.* beach nourishment. Sinks could include removal of sediment through suspension processes and offshore advection. Eq. (69) can be integrated seaward from a landward limit of no transport to any location, y

$$Q(y) - \int_0^y (\text{sources-sinks}) dy = \int_0^y \frac{\partial h}{\partial t} dy \qquad (70)$$

If only natural processes are involved and there are no gradients of longshore sediment transport, the terms on the left hand side of Eq. (70) represent the net rate of increase of sediment deficit as a function of offshore distance, y. For y values greater than the normal width, W_*, of the zone of active motion, the left hand side can be considered as representing the "ambient" deficit rate due to cross-shore sediment transport resulting from long-term disequilibrium of the profile and source and sink terms.

In attempting to apply Eq. (70) to the prediction of profile change and/or nourishment needs under a scenario of increased sea level rise, it is reasonable to assume that over the next several decades the ambient deficit rate (or surplus) of sediment within the active zone will remain constant. However, an increased rate of sea level rise will cause an augmented demand which can be quantified as $W_* \left[\left(\frac{dS}{dt} \right) - \left(\frac{dS}{dt} \right)_0 \right]$ in which $\left(\frac{dS}{dt} \right)_0$ is the reference sea level change rate during which time the ambient demand rate is established. Thus the active zone sediment deficit rate will be

New Deficit Rate

$$= \left[\int_0^{W_*} \frac{\partial h}{\partial t} dy \right]_0 + W_* \left[\left(\frac{dS}{dt} \right) - \left(\frac{dS}{dt} \right)_0 \right] - \frac{dV}{dt} \qquad (71)$$

in which dV/dt represents the nourishment rate and the subscript "0" on the bracket represents the reference period before increased sea level rise. In order to decrease the deficit rate to zero, the required nourishment rate is

POSSIBLE MECHANISM OF SEDIMENTARY EQUILIBRIUM
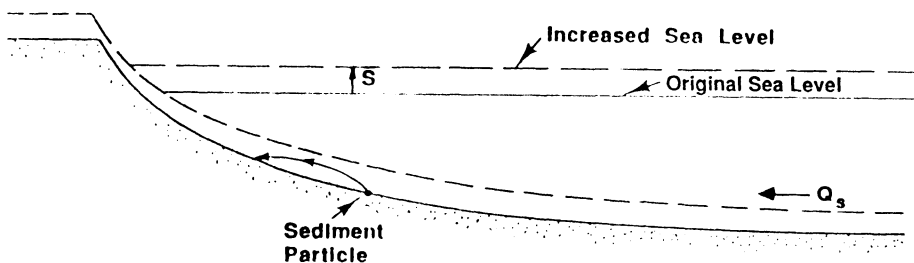
Subjected to a Given Statistical Wave Climate, A Sediment Particle of a Particular Diameter Is In Statistical Equilibrium When In a Given Water Depth

Thus When Sea Level Increases, Particle Moves Landward

Figure 32. Possible mechanism of sedimentary equilibrium (After Dean, 1987b).

$$\frac{dV}{dt} = \left[\int_0^{W*}\frac{\partial h}{\partial t}dy\right]_0 + W_*\left[\left(\frac{dS}{dt}\right) - \left(\frac{dS}{dt}\right)_0\right] \quad (72)$$

These models may assist in evaluating the vulnerability of various shoreline systems to increased rates of sea level rise.

Cross-Profile Volumetric Redistribution Due to Sea Level Rise

Eq. (13) was developed earlier to describe the shoreline change, Δy, due to a sea level rise, S. Associated with this recession is a cross-shore transfer of sediment from the upper to the lower portions of the profile. However there will be no net change of *volume* across the entire active profile. This statement would not hold, of course, if a portion of the eroded profile were peat or lagoonal muds that would be transported by suspension well beyond the normal limits of the active profile.

It is instructive to consider the change in volume that would be measured due to surveys extending out to a depth, h_s, which is less than the active profile depth, h_*. Referring to Figure 33a, the volumetric change per unit length due to profile equilibration as a result of sea level rise, S, must be considered for four regions:

$$V_A = -\int_{-B}^{h_s}\Delta y\ dh\ ,\ -B<h_s<-S$$

$$V_B = V_A(-S)-\int_{-S}^{h_s}\left[\Delta y+\left(\frac{h+S}{A}\right)^{3/2}\right]dh,$$

$$-S<h_s<0$$

$$V_C = V_B(0)+\int_0^{h_s}\left[-\Delta y+\left(\frac{h}{A}\right)^{3/2}\right.$$

$$\left.-\left(\frac{h+S}{A}\right)^{3/2}\right]dh, \quad (73)$$

$$0<h_s<h_*-S$$

$$V_D = V_C(h_*-S)+\int_{h_*-S}^{h_s}\left[-\Delta y+\left(\frac{h}{A}\right)^{3/2}\right.$$

$$\left.-W_*\right]dh,h_*-S<h_s<h_*-S+\Delta$$

The depth, h_c, at which the profiles cross will represent a maximum volume, V_{max}, and is given by

$$h_c = h_*\left[\frac{-\Delta y}{W_*}+\left(\frac{h_c}{h_*}\right)^{3/2}\right]^{2/3}-S \quad (74)$$

and must be solved by iteration. The maximum volume, V_{max}, which occurs at h_c is

$$V_{max} = -\Delta y\left(B+\frac{3}{5}h_c-\frac{2}{5}S\right)-\frac{2}{5}W_*S\left(\frac{h_c}{h_*}\right)^{3/2} \quad (75)$$

The height Δ can be shown to be

$$\Delta = h_*\left[\left(1+\frac{\Delta y}{W_*}\right)^{2/3} - 1+\frac{S}{h_*}\right] \quad (76)$$
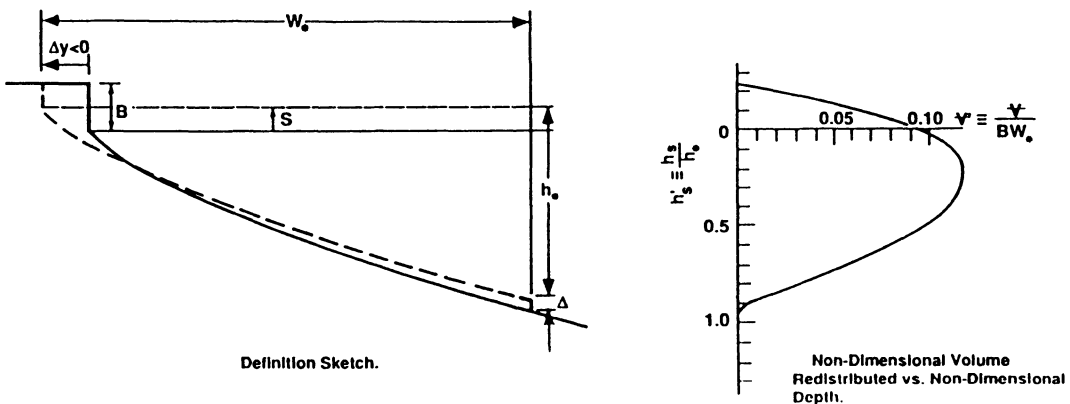
The above integration results can be cast into

Figure 33. Definition sketch and non-dimensional volume redistributed as a function of non-dimensional depth due to sea level rise, S. Case of $B/h_* = 0.25$, $S/B = 0.5$.

non-dimensional form with the following non-dimensional parameters $\Delta y' = \Delta y/W_*$, $h'_s = h_s/h_*$, $h'_c = h_c/h_*$, $\Delta' = \Delta/h_*$, $S' = S/B$, $B' = B/h_*$, and $V' = V/W_*B$.

The non-dimensional volumes are

$$V'_A = -\Delta y'\left(1+\frac{h'_s}{B'}\right), \quad -B'<h'_s<-S'B' \quad (77)$$

$$V'_B = -\Delta y'\left(1+\frac{h'_s}{B'}\right) - \frac{2}{5B'}(h'_s+S'B')^{5/2},$$
$$-S'B'<h'_s<0 \quad (78)$$

$$V'_C = -\Delta y'\left(1+\frac{h'_s}{B'}\right)$$
$$+ \frac{2}{5B'}[(h'_s)^{5/2} - (h'_s+S'B')^{5/2}], \quad (79)$$
$$0<h'_s<1-S'B'$$

$$V'_D = -\Delta y'\left(1+\frac{h'_s}{B'}\right) + \frac{2}{5B'}(h'_s)^{5/2}$$
$$- \left(\frac{h'_s}{B'}+S'\right) + \frac{3}{5B'}, \quad (80)$$
$$1 - S'B'<h'_s<1-S'B'+\Delta'$$

It can be shown by substituting the value of Δ' from Eq. (76) and $\Delta y'$ from Eq. (13) into Eq. (80), that $V'_D(h'_s = 1 - S'B' + \Delta') \equiv 0$ as would be expected since there has simply been a redistribution of the total volume in the profile rather than a net volume change.

To illustrate the volume changes that would be determined by surveying to various depths, h_s, consider the following example, $B' = B/h_* = 0.25$, $S' = S/B = 0.5$. For this case, the following results are obtained: $\Delta y' = \Delta y/W_* = -0.103$, $h'_c = h_c/h_* = 0.239$, $\Delta' = \Delta/h_* = 0.055$, $V'_{max} = V_{max}/(W_*B) = 0.118$.

The variation of the cross-shore volumetric transport versus depth below the elevated water level, S, is shown in Figure 33b for this example. It is seen as expected that the total volumetric change at $h = h_* + \Delta$ is zero.

It is of interest to compare the maximum volumetric change, V_{max}, with the volume deficit associated with a sea level rise, S. The latter quantity is simply W_*S. Thus this ratio, r, is

$$r \equiv \frac{V'_{max}W_*B}{W_*S} = \frac{V'_{max}}{S'}$$

and for our example

$$r = \frac{(0.118)}{0.5} = 0.236$$

Thus, the *maximum* volumetric survey error

that could occur due to the surveys not extending to a sufficient depth is approximately 25% of the volume deficit associated with the sea level rise.

It is also possible to develop *approximate* expressions describing the volumetric redistribution. First, we approximate the non-dimensional recession (Eq. (13)) by

$$\Delta y' \approx -\frac{S}{(h_*+B)} = -\frac{S'}{\left(1+\frac{1}{B'}\right)}$$

which for our example yields $\Delta y' = -0.100$ vs the complete equation result of -0.103. The approximate expression for h'_c is

$$h'_c = \frac{4}{9}\left(\frac{\Delta y'}{S'B'}\right)^2 \quad (81)$$

which for our case yields $h'_c = 0.301$ versus the complete equation result of 0.239. The value of Δ' obtained from the approximate value of $\Delta y'$ is $\Delta' = 0.057$ vs 0.055 obtained from the complete equation. Finally, the maximum non-dimensional volume, V'_{max}, is 0.1192 versus 0.1180 obtained from the full equation. In general, it is seen that for this example the approximations to the full equations are quite reasonable.

Trailing Beach Profile Signature Due to Sea Level Rise

If, as discussed by BRUUN (1962), and as implied by Eq. (15), the beach profile moves landward and upward in response to sea level rise, it is possible to infer a simple trailing beach profile signature, which can then be compared with measured cross-continental shelf profiles. The processes are complex due primarily to the landward boundary of the profile and the implicit assumption in Eq. (15) that the sand is transported only offshore. These potential shortcomings aside, Eq. (15) predicts that for each unit of vertical rise, the landward retreat of every element on the equilibrium beach profile will be, $W_*/(h_* + B)$, a value usually considered to be in the range of 50 to 100. Thus the trailing profile slope should be the inverse of this ratio. A comprehensive investigation of profiles may provide insight into con-

ditions under which Eq. (15) is most valid and/ or of the ratio $W_*/(h_* + B)$.

SUMMARY AND CONCLUSIONS

Equilibrium beach profile concepts provide a useful basis for application to a number of coastal engineering projects. In addition to addressing conditions at equilibrium, these concepts establish a foundation for considering the response of profiles out of equilibrium.

Based on analysis of numerous profiles representing laboratory and field scales, a reasonable approximate and useful form of a monotonic beach profile appears to be $h(y) = Ay^{2/3}$ in which h is the water depth at a distance, y, offshore and A is a scale parameter depending on sediment characteristics. Representations of the sediment scale parameter variation with sediment diameter and fall velocity are presented.

Methods are presented for quantifying the shoreline response due to elevated water levels and wave heights on natural and seawalled shorelines. Additionally, results are presented for calculating nourishment quantities for sand of uniform but arbitrary diameter. Depending on volumes and sizes of sediment added, three types of profiles can occur: intersecting, nonintersecting and submerged. The advantages of using coarser sand are quantified and equations are presented expressing the volume of a particular sand size required to yield a desired additional beach width. Many laboratory studies of beach profiles commence with a planar slope which could be much steeper or coarser than the overall equilibrium slope consistent with the sand size in the experiments. Applying equilibrium beach profile concepts, it is shown that five profile types relative to the initial profile can occur. Three of these types are erosional and two are accretional. Three of these profile types have been identified in laboratory studies. Conditions under which a profile type will occur are quantified and all results including shoreline change are incorporated into a single graphical representation.

The volumetric redistribution of sediment across the profile due to sea level rise is examined in detail and compared with the total sediment "demand" as a result of the sea level rise. An application is the possible error if the survey does not extend over the full depth of effec-tive motion. It is shown that the maximum error is only a fraction of the sediment "demand".

The effects of sea level rise on nourishment needs are evaluated for cases with and without onshore sediment transport across the continental shelf. It is shown that the sediment volumes required to maintain a shoreline position vary directly with wave height and sea level rise rates and inversely with profile slopes.

It is hoped that the results presented herein will provide guidance for coastal engineering projects and serve as a framework for interpretation of project performance and behavior of natural beach systems.

ACKNOWLEDGEMENTS

LITERATURE CITED

AUBREY, D.G., 1979. Seasonal Patterns of Onshore/ Offshore Sediment Movement. *Journal of Geophysical Research,* 84(C10), 6347–6354.

AUBREY, D.G.; INMAN, D.L., and NORDSTROM, C.E., 1977. Beach Profiles at Torrey Pines, CA. *Proceedings of the Fifteenth International Conference on Coastal Engineering,* American Society of Civil Engineers, pp. 1297–1311.

BAGNOLD, R.A., 1946. Motion of Waves in Shallow-Water—Interaction Between Waves and Sand Bottoms. *Proceedings Royal Society,* 187 (Series A), 1–15.

BOWEN, A.J.; INMAN, D.L., and SIMMONS, V.P., 1968. Wave Set-Down and Wave Set-Up. *Journal of Geophysical Research,* 73(8), 2569–2577.

BRUUN, P., 1954. Coast Erosion and the Development of Beach Profiles. *Technical Memorandum No. 44,* Beach Erosion Board.

BRUUN, P., 1962. Sea Level Rise as a Cause of Shore Erosion. *Journal of Waterway, Port, Coastal and Ocean Engineering,* American Society of Civil Engineers, 88, 117–130.

CHIU, T.Y., 1977. Beach and Dune Response to Hurricane Eloise of September 1975. *Proceedings of the*

Specialty Conference on Coastal Sediments '77, American Society of Civil Engineers, pp. 116–134.

DALRYMPLE, R.A., and THOMPSON, W.W., 1976. Study of Equilibrium Profiles. *Proceedings of the Fifteenth International Conference on Coastal Engineering,* American Society of Civil Engineers, 1277–1296.

DEAN, R.G., 1973. Heuristic Models of Sand Transport in the Surf Zone. *Proceedings of the Conference on Engineering Dynamics in the Surf Zone,* Institution of Civil Engineers, Australia, Sydney, pp. 208–214.

DEAN, R.G., 1977. Equilibrium Beach Profiles: U.S. Atlantic and Gulf Coasts. Department of Civil Engineering, *Ocean Engineering Report No. 12,* University of Delaware, Newark, Delaware.

DEAN, R.G., 1987a. Coastal Sediment Processes: Toward Engineering Solutions. *Proceedings of the Specialty Conference on Coastal Sediments '87,* American Society of Civil Engineers, pp. 1–24.

DEAN, R.G., 1987b. Additional Sediment Input to the Nearshore Region. *Shore and Beach,* 55(3–4), 76–81.

DEAN, R.G., and MAURMEYER, E.M., 1983. Models for Beach Profile Response. *In:* KOMAR, P.D., (ed.), *CRC Handbook of Coastal Processes and Erosion.* Boca Raton, CRC Press, Chapter 7, pp. 151–166.

EAGLESON, P.S.; GLENNE, B., and DRACUP, J.A., 1963. Equilibrium Characteristics of Sand Beaches. *Journal of Hydraulics Division,* American Society of Civil Engineers, 89(HY1), pp. 35–57.

HAYDEN, B.; FELDER, W.; FISHER, J.; RESIO, D.; VINCENT, L., and DOLAN, R., 1975. Systematic Variations in Inshore Bathymetry. Department of Environmental Sciences, *Technical Report No. 10,* University of Virginia, Charlottesville, VA.

HOFFMAN, J.S.; KEYES, D., and TITUS, J.G., 1983. *Projecting Sea Level Rise; Methodology, Estimates to the Year 2100 and Research Needs.* U.S. Environmental Protection Agency, Washington, D.C.

HUGHES, S.A., 1983. Movable Bed Modeling Law for Coastal Dune Erosion. *Journal of Waterway, Port, Coastal and Ocean Engineering,* 109(2), 164–179.

KEULEGAN, G.H., and KRUMBEIN, W.C., 1949. Stable Configuration of Bottom Slope in a Shallow Sea and Its Bearing on Geological Processes. *Transactions of American Geophysical Union,* 30(6), 855–861.

KRIEBEL, D.L., 1982. Beach and Dune Response to Hurricanes, M.S. Thesis, Department of Civil Engineering, University of Delaware, Newark, Delaware.

KRIEBEL, D.L., 1986. Verification Study of a Dune Erosion Model. *Shore and Beach,* 54(3), 13–21.

KRIEBEL, D.L., and DEAN, R.G., 1984. Beach and Dune Response to Severe Storms. *Proceedings of the Nineteenth International Conference on Coastal Engineering,* American Society of Civil Engineers, pp. 1584–1599.

KRIEBEL, D.L., and DEAN, R.G., 1985. Numerical Simulation of Time-Dependent Beach and Dune Erosion. *Coastal Engineering,* 9(3), 221–245.

LARSON, M., 1988. Quantification of Beach Profile Change. *Report No. 1008,* Department of Water Resources Engineering, Lund University, Lund, Sweden.

LARSON, M., and KRAUS, N.C., 1989. SBEACH: Numerical Model for Simulating Storm-Induced Beach Change—Report 1: Empirical Foundation and Model Development. *Technical Report CERC-89-9,* Coastal Engineering Research Center, Waterways Experiment Station, Vicksburg, Mississippi.

MOORE, B.D., 1982. Beach Profile Evolution in Response to Changes in Water Level and Wave Height. Masters Thesis, Department of Civil Engineering, University of Delaware.

NODA, E.K., 1972. Equilibrium Beach Profile Scale Model Relationship. *Journal Waterways, Harbors and Coastal Engineering Division,* American Society of Civil Engineers, pp. 511–528.

PHILLIPS, O.M., 1966. *The Dynamics of the Upper Ocean.* Cambridge, England: Cambridge University Press, 261p.

SAVILLE, T., 1957. Scale Effects in Two-Dimensional Beach Studies. *Transactions of the Seventh General Meeting of the International Association of Hydraulic Research,* Vol. 1, p. A3-1 to A3-10.

STIVE, M.J.F., and WIND, H.G., 1986. Cross-Shore Mean Flow in the Surf Zone. *Coastal Engineering,* 10(4), 325–340.

SUH, K., and DALRYMPLE, R.A., 1988. Expression for Shoreline Advancement of Initially Plane Beach. *Journal of Waterway, Port, Coastal and Ocean Engineering,* American Society of Civil Engineers, 114(6), 770–777.

SUNAMURA, T., and HORIKAWA, K., 1974. Two-Dimensional Beach Transformation Due to Waves. *Proceedings of the Fourteenth International Conference on Coastal Engineering,* American Society of Civil Engineers, pp. 920–938.

SWART, D.H., 1974. A Schematization of Onshore-Offshore Transport. *Proceedings of the Fourteenth International Conference on Coastal Engineering,* American Society of Civil Engineers, pp. 884–900.

SVENDSEN, I.A., 1984. Mass Flow and Undertow in a Surf Zone. *Coastal Engineering,* 8, 347–365.

VAN HIJUM, E., 1975. Equilibrium Profiles of Coarse Material Under Wave Attack. *Proceedings of the Fourteenth International Conference on Coastal Engineering,* American Society of Civil Engineers, pp. 939–957.

VELLINGA, P., 1983. Predictive Computational Model for Beach and Dune Erosion During Storm Surges. *Proceedings of the Specialty Conference on Coastal Structures '83,* American Society of Civil Engineers, pp. 806–819.

WEISHAR, L.L., and WOOD, W.L., 1983. An Evaluation of Offshore and Beach Changes on a Tideless Coast, *Journal of Sedimentary Petrology,* 53(3), 847–858.

WINANT, C.D.; INMAN, D.L., and NORDSTROM, C.E., 1975. Description of Seasonal Beach Changes Using Empirical Eigenfunctions. *Journal of Geophysical Research,* 80(15), 1979–1986.

ZENKOVICH, V.P., 1967. *Processes of Coastal Development.* Editor: J.A. Steers. Edinburgh: Oliver and Boyd, 738p.

□ RÉSUMÉ □

La compréhension des profils d'équilibre est utile à bon nombre de projets d'ingénierie côtière. A partir d'équations empiriques entre un paramètre d'échelle et la taille du sédiment ou sa vitesse de chute, on peut calculer le profil d'équilibre. La forme la plus utilisée est de la forme: $h(y) = A\,y^{2/3}$ où h est la profondeur à une distance y du rivage et A un paramètre dépendant du sédiment. Les expressions du changement de la position du rivage sont donnés pour des niveaux de la mer arbitraires et diverses hauteurs de la houle. L'application des concepts de profil d'équilibre à des modifications du profil côté mer d'une digue tient compte des effets de la modification du niveau de la mer et des hauteurs de la houle. Pour des vagues d'une hauteur donnée et un niveau de l'eau croissant, la profondeur adjacente à la digue croît d'abord, puis décroît jusqu'à zéro (houle brisant sur la digue). Le recul de rivage, les conséquences de la hausse du niveau de la mer et de la hauteur de la houle sont examinés. Ainsi, l'effet de l'établisse-ment de la houle sur le recul est faible, comparé à celui des marées de tempête. L'évolution des profils à partir d'une pente uniforme peut doner 5 types différents qui dépendent de la pente initiale, des caractères du sédiment, de la hauteur de la berme et de la profondeur de la redistribution active des sédiments. La réduction du volume de sable nécessaire à l'engraissement de la plage par une buse placée au large est examinée pour un sédiment quelconque et toutes les combinaisons. Quand les plages sont nourries, il résulte trois types de profils: 1) profils submergés où les sédiments d'apport sont plus petits que ceux d'origine: tous les sédiments s'équilibrent sous l'eau, sans élargissement de la plage sèche; 2) profils ne se recoupant pas, où le matériau d'apport est localisé sur le bas de plage et repose sur le profil originel à cet endriot; 3) profils se recoupant: le sable d'apport est plus gros que celui d'origine et recoupe le profil originel. Des équations et des graphes donnent la figure de la largeur de la plage sèche pour différents volumes de sable et des tailles variées de sédiments d'origine. Les redistributions volumétriques de matériaux au large, dues à la montée relative du niveau de la mer en fonction de la profondeur sont utiles à l'interprétation de la cause du retrait du rivage. S'il y a seulement transport vers le large, et que l'on considère aussi les profils actifs, le changement volumétrique net est nul. On montre que le changement maximum de volume dû à la redistribution transversale des sédiments de la plage n'est qu'une fraction du produit de la dimension du profil vertical et du retrait du rivage. Cet article présente aussi plusieurs applications des profils d'équilibre à des problèmes d'ingénierie côtière.—*Catherine Bressolier-Bousquet, Géomorphologie EPHE, Montrouge, France.*